Макрогетероциклы
http://macroheterocycles.isuct.ru

DOI: 10.6060/mhc160529z

Deactivation of Excited States in Nanostructures Containing Cu–Porphyrin Subunit

Eduard I. Zenkevich

National Technical University of Belarus, Department of Information Technologies and Robotics, 220013 Minsk, Belarus
E-mail: zenkev@tut.by

Here, we present a semi-review of mutual Belarussian-German collaboration in the field of supramolecular chemistry and photophysics of tetrapyrrole compounds of various types: porphyrin chemical dimers, self-organized multiporphyrin complexes, ordered aggregates of photosynthetic pigments and nanoassemblies based on semiconductor CdSe/ZnS quantum dots and porphyrins. A special attention is paid to various nanostructures containing Cu-porphyrin subunits. Based on steady-state and time-resolved measurements, spectral properties as well as pathways and dynamics of non-radiative relaxation processes with participation of singlet and triplet excited states (energy transfer, photoinduced electron transfer, exchange d-π effects) are the subject of the analysis upon variation of the temperature (77-295 K) and polarity of the solvent. Finally, we consider recent results on "Quantum Dot-Porphyrin" nanoassemblies showing that self-assembly of only one Cu-porphyrin molecule with one CdSe/ZnS quantum dot modifies not only the photoluminescence intensity of quantum dot but creates new energetically clearly distinguishable electronic states opening additional effective relaxation pathways.

Keywords*:* Porphyrins, porphyrin chemical dimers, self-organized multiporphyrin complexes, polymeric ordered chlorophyll aggregates, nanoassemblies "semiconductor quantum dots-porphyrins", deactivation of singlet and triplet excited states, energy/electron transfer.

Дезактивация возбужденных состояний в наноструктурах с участием Cu–порфирина как составляющего фрагмента

Э. И. Зенькевич

Белорусский национальный технический университет, Факультет информационных технологий и робототехники, 220013 Минск, Беларусь
E-mail: zenkev@tut.by

На основании стационарных, пикосекундных кинетических измерений и спектроскопии одиночных нанообъектов проведен сравнительный анализ путей и механизмов безызлучательных релаксационных процессов (перенос энергии/электрона, обменные d-π эффекты и др.) для различных наноструктур, содержащих Cu-порфирин: химические димеры порфиринов, самоорганизованные мультипорфириновые комплексы, упорядоченные агрегаты фотосинтетических пигментов, а также наноансамблей на основе полупроводниковых квантовых точек CdSe/ZnS и Cu-порфиринов.

Ключевые слова: Порфирины, химические димеры порфиринов, самоорганизованные мультипорфириновые комплексы, полимерные упорядоченные хлорофилловые агрегаты, наноансамбли на основе полупроводниковых квантовых точек, дезактивация синглетных и триплетных возбужденных состояний, перенос энергии/электрона.

Introduction

At present, supramolecular chemistry in solutions, films and on heterogeneous carriers presents itself a highly interdisciplinary field of nanotechnology covering the chemical, physical, and biological features of chemical species held together and organized by means of intermolecular binding interactions of various nature.[1-3] The most important source of inspiration for self-assembly strategies is natural photosynthesis (the biological world) in which the generation of complex, multicomponent three-dimensional structures involve intramolecular, as well as intermolecular and interfacial interactions.[4-9] Correspondingly, a significant interest of numerous scientific groups is devoted to the design and investigation of biomimetic models based on tetrapyrrole compounds that fold or self-assemble predictably in order to form multicomponent well-defined arrays with effective energy transfer and charge separation like in photosynthetic objects *in vivo*.[10-22] On the other hand, there are many promising self-organized systems or nanoassemblies (including even organic-inorganic counterparts) which offer exciting opportunities for the engineering and preparation of various man-made molecular nanodevices in the modern fields of molecular electronics (photoinduced molecular switches, photonic wires, solar cells, optoelectronic gates, information storage, *etc*.) and nanobiophotonics (nanoprobes for biomedical imaging, biosensing and photodynamic therapy of cancer, *etc*).[23-32] In this respect, the 2014 Nobel Prize in chemistry (E. Betzig, S.W. Hell and W.E. Moerner) devoted to the recent revolution in super-resolution optical microscopy opened a new and extremely wide range for applications of self-organized nanoassemblies of various composition and morphology in optical microscopy and bioimaging. Concluding, nanotechnology is playing a pivotal role in advancing Nano/Bio/Info technology by creating new interfaces between multiple disciplines.

It should be mentioned, that the main problem is the understanding presumably of how the multiple components by various nature and composition will interact and function as a whole in any given system. At the moment, the majority of conformationally restricted, structurally and energetically well-defined multiporphyrin moieties have been used in order to better understand factors and mechanisms which control the efficiency and directionality of the excitation energy relaxation pathways (presumably energy/electron transfer) taking place without diffusion limitations. A large body of interesting and important results obtained in this field (even when only concentrating on basic aspects and reported in the 1990-2000) has been described and discussed in earlier comprehensive reviews and in those fresh cited above.

In this paper, we would like to present and discuss some relatively rare relaxation processes in multicomponent nanostructures including Cu containing tetrapyrrolic macrocycles which make these nanoassemblies more special. Before we turn to the discussion of our results, in the following we will summarize shortly the basic ideas what should be taken into account. The analysis of data presented in literature[10,13,17-19,21,27,33-41, and ref. herein] shows that using a variety of central metal ions in tetrapyrrolic ring provides the possibilities of the formation of multiporphyrin systems of different structure and controlled photophysical and photochemical properties that govern the realization of ET or PET processes. For instance, assembly of porphyrins via non-covalent metal-ligand bonds provides a synthetically elegant route to a wide structural variation of multiporphyrin systems including both qualitative and quantitative aspects of the composition (homo- and heterodimers, triads, pentads and more complex arrays). On the other hand, in such hybrid multiporphyrin donor-acceptor systems, the introduction of various central metal ions may change spectral-kinetic parameters and redox properties of the corresponding subunits, and thus it is possible to control and tune the directionality, efficiency and rates of the competing energy transfer (ET) and photoinduced electron transfer (PET) processes taking place in these nanoassemblies.

Correspondingly, it follows from numerous results presented in literature that, particularly, for hybrid Zn(II) porphyrin-free base porphyrin chemical dimers with various spacers ET processes are distance and orientation dependent. Two major mechanisms for ET with participation of excited S_1 and T_1 states have been identified in these dimers, that is long-distant inductive-resonant mechanism without the direct contact of *D-A* components,[42,43] and exchange-resonant mechanism realized via spatial overlap of interacting subunits.[44,45] In addition, some specific factors need to be taken into account upon the analysis of ET dynamics in closely spaced multiporphyrin systems: electronic couplings via bridge in the directed energy migration, through-space Coulomb interaction in optimization of energy transfer in confined molecular assemblies, distributed transition monopole effects in electronic excitation interactions, excitonic effects.

Metaloporphyrin-free base hybrid dimers (with diamagnetic Zn, Mg ions presumably) covalently linked via rigid or flexible spacers of various nature as well multicomponent systems on their basis have been usefully employed also to test numerous theoretical models describing PET. It has been shown that the intracomplex PET may take place in a wide time-scale up to ps/fs regime depending on the energy of donor locally excited singlet (S_1) and triplet (T_1) states, redox properties of interacting *D-A* components, their mutual geometry and *D-A* intercenter distance as well as temperature and polarity of the solvent. In addition, for a set of porphyrin hybrid dimers, PET rate constants are essentially influenced by the spacer nature (electronic properties of chemical bond, the energy of spacer excited states, geometry and flexibility) as well as the additional coordination of porphyrin central metal ion by various extra-ligands. In the result, the interplay of all these factors determines the possible pathways and mechanisms of the PET in the given chemical dimer (theoretically considered as sequential "through-bond" or "through-space" mechanisms,[46-49] superexchange coupling through the bridge.[50,51]

Nevertheless, in comparison with multiporphyrin arrays involving subunits with diamagnetic metal ions (discussed above), the photochemistry of hybrid nanoassemblies having tetrapyrrolic counterparts with central paramagnetic metal ions, for instance Cu(II), is rather complex because of presence of unpaired d-electron in central metal. In the case of monomeric Cu(II)-porphyrins, it is well-documented[52-58] that the metal half-filled $d_{x^2-y^2}$ orbital of Cu ion lies in the

energy scale between the porphyrin macrocycle HOMOs $a_{1u}(\pi)$ and $a_{2u}(\pi)$ and LUMO $e_g(\pi^*)$. Exchange interactions of Cu unpaired electron with π-electrons of the porphyrin ring lead to the splitting of the porphyrin triplet state T_1 into "trip-doublet" ($^2T_1$) and "trip-quartet" ($^4T_1$) states with the corresponding energies (see Scheme 1):[52]

$$E(^2S_1)=E(^2\psi_1)-E(^2\psi_0)=\varepsilon_b-\varepsilon_a-J_{ab}+2K_{ab}=E(S_1),$$

$$E(^2T_1)=E(^2\psi_2)-E(^2\psi_0)=\varepsilon_b-\varepsilon_a-J_{ab}+(1/2)\times(K_{am}+K_{bm})=$$
$$=E(T_1)+(1/2)\times(K_{am}+K_{bm}), \quad (1)$$

$$E(^4T_1)=E(^4\psi_2)-E(^2\psi_0)=\varepsilon_b-\varepsilon_a-J_{ab}-(1/2)\times(K_{am}+K_{bm})=$$
$$=E(T_1)-(1/2)\times(K_{am}+K_{bm}),$$

where ε_i are orbital energies of excited (b) and ground (a) states, J_{ab} is Coulomb integral (the energy of electron repulsion), $K_{am}+K_{bm}$ are exchange d-π integrals characterizing the interaction of (a) and (b) states with d-electron (m-state). It follows from Eq. (1) that for monomeric Cu(II)-porphyrins the energy of the "sing-doublet" state $^2S_1$ is the same practically compared to that for usual metaloporphyrin. The energy gap $\Delta E=E(^2T_1)-E(^4T_1) \approx 150-700$ cm^{-1} depends on exchange d-π integrals (K_{am} + K_{bm}) and porphyrin side substituents. As far as $K_{bm}>>K_{am}$,[52] exchange interactions between excited molecular orbital of b-state and unpaired d-electron is stronger essentially compared to those between the non-excited molecular orbital of a-state and d-electron thus leading to $\Delta E=E(^2T_1)-E(^4T_1) \approx K_{bm}$. Correspondingly, luminescence of Cu-porphyrins is a function of temperature in the conditions of Boltzman distribution between $^2T_1$ and $^4T_1$ states, and may take place from $^2T_1$ state (room temperature) or $^4T_1$ state (low temperatures). In its turn, partially allowed character of the non-radiative $^2S_1 \sim\sim> ^2T_1$ intersystem crossing within time of τ_{ISC}~8-10 ps results in the strong fluorescence quenching observed for Cu-porphyrins.[88]

In addition, because of the non-zero electronic interactions between $^2S_1$- and $^2T_1$-states the formally spin-allowed transition $^2S_0 \rightarrow ^2T_1$ in absorption borrows the intensity (via exchange d-π interactions) from fully allowed $^2S_0 \rightarrow ^2S_1$ transition,[52] and the corresponding oscillator strength (f) of a such singlet-triplet $^2S_0 \rightarrow ^2T_1$ transition is determined by[59]

$$f\left(^2S_0 \rightarrow ^2T_1\right)=\frac{3}{4}\left[\frac{K_{bm}-K_{am}}{E\left(^2S_1\right)-E\left(^2T_1\right)}\right]^2 \cdot f\left(^2S_0 \rightarrow ^2S_1\right) \approx$$
$$\approx \frac{3}{4}\left[\frac{K_{bm}}{E\left(^2S_1\right)-E\left(^2T_1\right)}\right]^2 \cdot f\left(^2S_0 \rightarrow ^2S_1\right) \quad (2)$$

Correspondingly, the direct observation of such transitions in absorption for Cu-porphyrins in near IR-range and estimation of their parameters for the first time[60] was the real background for the experimental estimation of the energy of the "trip-doublet" $^2T_1$-state as well the energy gap $\Delta E=E(^2T_1)-E(^4T_1)$ and determination of the multiplicity of the electronic state responsible for the phosphorescence.

Finally, because of the presence Cu half-filled $d_{x^2-y^2}$ orbital, several charge transfer (π,d) and (d,π*) transitions (CT) are possible. It means that the existence of such CT states may lead to the corresponding quenching of luminescence from $^2T_1$ and $^4T_1$ states for Cu-porphyrins. Depending on porphyrin structure, temperature, polarity and coordination properties of the solvent possible mechanisms of this quenching are as follows: thermal activation of upper-lying CT states, the increase of non-radiative transition rate constants due to the perturbation by a close-lying CT states, the direct electron transfer to low-lying CT states of (π,d) or (d,π*) nature.[53,57,58]

With these backgrounds in mind, the important question arises: what happens with excited states (namely, S_1 and T_1) of tetrapyrrolic subunits being coupled with adjacent Cu-porphyrins via various spacers in nanoassemblies of a given nature and morphology. In this respect, the main aim of the present paper is the comparative analysis of the main regularities of deactivation processes in such systems of various complexities based on our own experimental results as well as taking into account basic findings obtained in other groups. We will start with considering the photochemistry of (H_2P+CuP), (ZnP+CuP) hybrid porphyrin dimers in the comparison with the corresponding symmetrical homodimers, (H_2P+H_2P), (ZnP+ZnP), having various structures of porphyrin macrocycles as well as spacers of various electronic nature and rigidity in a temperature range of 295-77 K. The principal interest is also to evaluate electronic communications for symmetrical (CuP+CuP) dimers with various spacers and having two central Cu(II) ions with unpaired d-electrons in both halves. To our knowledge, these effects for various types of symmetrical (CuP+CuP) dimers have not been comparatively discussed yet. Further, the specificity of long-distant exchange d-π interactions will be elucidated for more complex multiporphyrin self-assembled arrays:

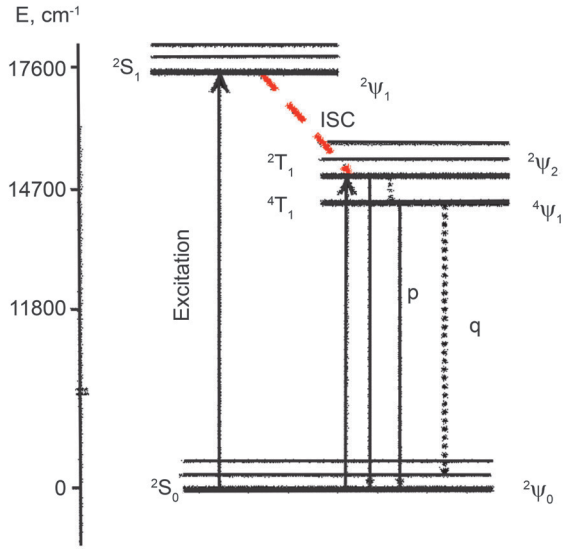

Scheme 1. Diagram of energy levels for Cu-octaethylporphyrin molecule in toluene at ambient temperature. Solid black arrows show absorption and radiative intramolecular transitions, dashed arrows show non-radiative transitions, red dashed arrow shows the non-radiative intersystem crossing process.

pentads and larger complexes with well-defined geometry and containing Cu-porphyrin subunit. The manifestation of exchange d-π effects will be demonstrated also for polymeric ordered aggregates of photosynthetic pigments (with strong excitonic coupling) having admixture of Cu-pheophytin molecules. Finally, we will present our recent results on "quantum dot-porphyrin" nanoassemblies showing that self-assembly of only one Cu-porphyrin molecule with one CdSe/ZnS quantum dot modifies not only the photoluminescence intensity of quantum dot but creates new energetically clearly distinguishable electronic states opening additional effective relaxation pathways.

We do not claim to review all published results in this field because this is clearly beyond the scope of this paper. The idea of this paper is not a thorough theoretical description of all the relaxation processes in multicomponent structures, which would be too early given some open problems as well as some specific structural aspects. Instead, the intent is to provide a representative description of manifestation and specificity of long-distant exchange d-π interactions for various nanostructures containing Cu-porphyrin subunits taken into account some first papers as well as some of our recent results. In some respect, this paper provides the data for a further development of defined multicomponent structures for exploitation as artificial light-harvesting complexes, electro- and photochemical devices, nanosensors, *etc*.).

Experimental

Materials

Covalently linked porphyrin dimers. Synthesis, purification, and determination of the structure of precursor monomeric porphyrin molecules as well as the corresponding chemical homo- and heterodimers (free bases, Zn and Cu complexes) were performed by Dr. A. Shulga in B.I. Stepanov Institute of Physics, National Academy of Sciences of Belarus (Minsk) and described in details together with their optical properties in our earlier publications. In this paper, the subject of the discussion will be the dimers in which tetrapyrrolic subunits are covalently linked via spacers of various nature: i) ethane-bisporphyrins with a single -CH_2-CH_2- via *meso*-positions,[34,61-67] ii) cyclodimers where cyclopentaneporphyrin molecules are coupled via isocycles,[68-73] and iii) chemical dimers of octaethylporphyrins with the phenyl bridge via *meso*-positions.[17,18,27,74-76] It should be noted that in order to clarify spectral-kinetic properties that are characteristic for the dimers namely, we have especially prepared and characterized the precursor monomeric species with side substituents of the same nature and in the same positions like the corresponding spacers.

For the reader convenience, the optimized structures of the studied dimers as well as of other multicomponent complexes discussed in the paper are presented in the corresponding parts of the text describing their photophysical properties and excited states relaxation.

Self-assembled multiporphyrin complexes. Formation of such complexes is based on the simultaneous use of covalent and non-covalent approaches that was generally proposed first by J.-M. Lehn.[1] Correspondingly, we have succeeded to obtain (by directed way) highly organized and relatively rigid multicomponent tetrapyrrole assemblies in solutions and polymeric films.[21,27,38,74,77-80] The covalent stage includes the synthesis of Zn-porphyrin chemical dimers or trimers with a phenyl spacer in *meso*-position. The second stage presents itself the self-assembly of these dimers or trimers with *meso*-pyridyl substituted porphyrins (free bases or Cu-complexes) via non-covalent binding interactions (two-fold extra-ligation effect following the "key-lock" principle). The "key-lock" principle is based on the complexation of central Zn ions of porphyrin chemical dimers or trimers with suitable extra-ligands (tetrapyridyl substituted tetrapyrrolic macrocycles, in our case) via two-fold non-covalent coordination.[74,77,81-84] One principal moment should be taken into account in this case: the matching geometry between nitrogen atoms in meso-pyridyl containing extra-ligands and Zn-Zn distance in the dimers and trimers plays the essential role in the formation of triads and pentads with relatively well-defined conformational rigidity.[74,77,80] The structure of the complexes under discussion will be shown below.

Ordered aggregates of photosynthetic pigments. We have shown that a small amount of bifunctional linker molecule (like dioxane) plays the directed role in the formation of stable polymeric ordered aggregates of photosynthetic pigments (chlorophylls *a* and *b*, protochlorophyll or bacteriochlorophyll) being previously dissolved in solvents with poor solubility (such as water or 3-methylpentane).[85-88] The size and the morphology of these aggregates and their spectroscopic properties (polarized fluorescence and high optical activity) depend strongly on the linker molecule, concentration, ratio of the solvent mixture and temperature.[87-89] In binary mixture of solvents we realized conditions where the formation of mixed aggregates of different molecules but having the general structural elements, was thermodynamically more preferable.[85,87] The dioxane as a linker molecule keeps, according to calculations, the interplane distance between the adjacent pigment molecules at about 7 Å. The consequence of inclusion of Cu-pheophytin molecules into mixed aggregates will be discussed in a separate section.

Nanoassemblies based on semiconductor quantum dots CdSe/ZnS and porphyrin molecules (free bases and Cu-complexes). The *n*-trioctylphosphine oxide (TOPO) caped CdSe/ZnS quantum dots (QD) with an inorganic ZnS shell were used to form QD-porphyrin nanoassemblies in non-polar solvents at ambient temperature. In this case, like for multiporphyrin complexes (described above), a controllable formation of "QD-Porphyrin" nanoassemblies have been realized as a surface passivation of CdSe/ZnS ODs by tetra-*meso*-pyridyl substituted porphyrins (free base and/or Cu-complex) in titration experiments.[29,90-99] It is well-known from chemical background that the 3d transition metal Zn^{2+} ion (of ZnS shell) has empty $3d^{10}$ orbital while heteroatom N-pyr of the porphyrin *meso*-pyridyl ring is a very good e-donor having an unshared electron pair. Thus, in this case a "key-lock" principle is realized via one- or two-fold non-covalent coordination Zn….N-pyr. Synthesis and characterization of *meso*-pyridyl containing porphyrins have been described in above cited papers.[74,77]

Solvents

For dimers, multiporphyrin complexes and QD-porphyrin nanoassemblies, toluene (Aldrich, spectroscopic grade), was used as basic solvent at 295 K. Low-temperature measurements (77 K) were carried out in a mixture of methylcyclohexane-toluene (6:1, spectroscopic grade, Fluka SeccoSolv dried over a molecular sieve) or in the solvent mixture of diethyl ester-petroleum ester-isopropanol 5:5:2 (EPIP both forming an optical transparent rigid glass matrix at these conditions. For aggregates of photosynthetic pigments distilled water-dioxane (4:1) mixture was used for measurements at ambient temperature, experiments at 77 K have been carried out in the mixture of 3-methylpentane-dioxane (10000:1). For low-temperature experiments a home-made cryostat was used.

Spectral and Kinetic Measurements

Electronic absorption spectra were recorded on Shimadzu UV-3101PC and Varian Cary 500 Scan spectrophotometers. The static fluorescence and excitation spectra were recorded on a Shimadzu RF-5001PC spectrofluorimeter. Corrected steady-state fluorescence and phosphorescence spectra at various temperatures were measured also on a laboratory spectral-luminescent set-up, equipped with a personal computer. It is based on two grating monochromators MDR-23. The operating spectral region was from 200 nm to 1100 nm, and the exciting light sources were high pressure xenon lamp DKsSh-3000 with water cooling system xenon or an argon laser. Phosphorescence decays were measured at 0-0 bands maxima of phosphorescence spectra by the pulse method using the second harmonic of the YAG:Nd^{3+} pulse solid laser (λ_{ex}=532 nm, the experimental response $\Delta t_{1/2}$=15 ns FWHM) for the excitation and the recording system based on monochromator, a photomultiplier FEU-83 and a digital oscilloscope S9-27 equipped with a personal computer. Time-resolved PL measurements on ensembles were performed in a time-correlated single photon counting (TCSPC) mode under right-angle geometry using a laboratory spectrofluorometer equipped with computer module TCC900 (Edinburg Instruments) and light emitting diodes. Fluorescence and phosphorescence measurements have been carried out, using samples having a concentration of ~10^{-6}-10^{-5} M. In liquid solutions at 293 K, triplet state decays were measured using a laboratory experimental set-up with laser excitation (the second harmonic of the YAG:Nd^{3+} pulse solid laser, λ_{ex}=532 nm, $\Delta t_{1/2}$=15 ns FWHM). Time and spectrally resolved single QD experiments have been carried out with a home-built set-up.[97,100,101] All photophysical measurements were completed within 1-2 hours following preparation. Additional experimental details are presented in the corresponding papers cited for every class *f* compounds being studied.

Results and Discussion

Photochemistry of Hybrid Porphyrin Dimers with Various Spacers

Historically, the first paper on this subject has been published in 1972.[102] Interchromophoric interactions in double porphyrin molecules (containing Cu, Zn or Co) linked via amide groups, CO-XH-R-NH-CO (where R is either an ethylene or *p*-phenylene group) have been studied in rigid solutions of 2-methyltetrahydrofurane at 77 K. For the ethylene bridged dimer the average distance between the metals of the chromophores is ~5 Å, while in the phenylene-bridged double porphyrins there is no overlap and the centers of the chromophores are separated by ~10 Å. Intramolecular energy transfer from the zinc triplet state to that of the copper trip-doublet is manifested in shortening of the zinc porphyrin triplet state lifetime in the ethylene bridged dimers. It was proposed also that quenching mechanism may be connected with paramagnetic effect by the neighboring Cu atom enhancing the intersystem crossing rate. Lack of any evidence for chromophore interaction in the phenylene-linked porphyrins is due to low overlap. Later on, for Zn-porphyrin+Cu-porphyrin chemical dimers, the absence of the non-radiative singlet-singlet energy transfer CuP→ZnP[103] was explained by rapid intersystem crossing known for monomeric copper porphyrin molecules.[54] First results of our group in this field have been obtained for mixed ethanebisporphyrins in 1983-1984.[62,63,105] In the

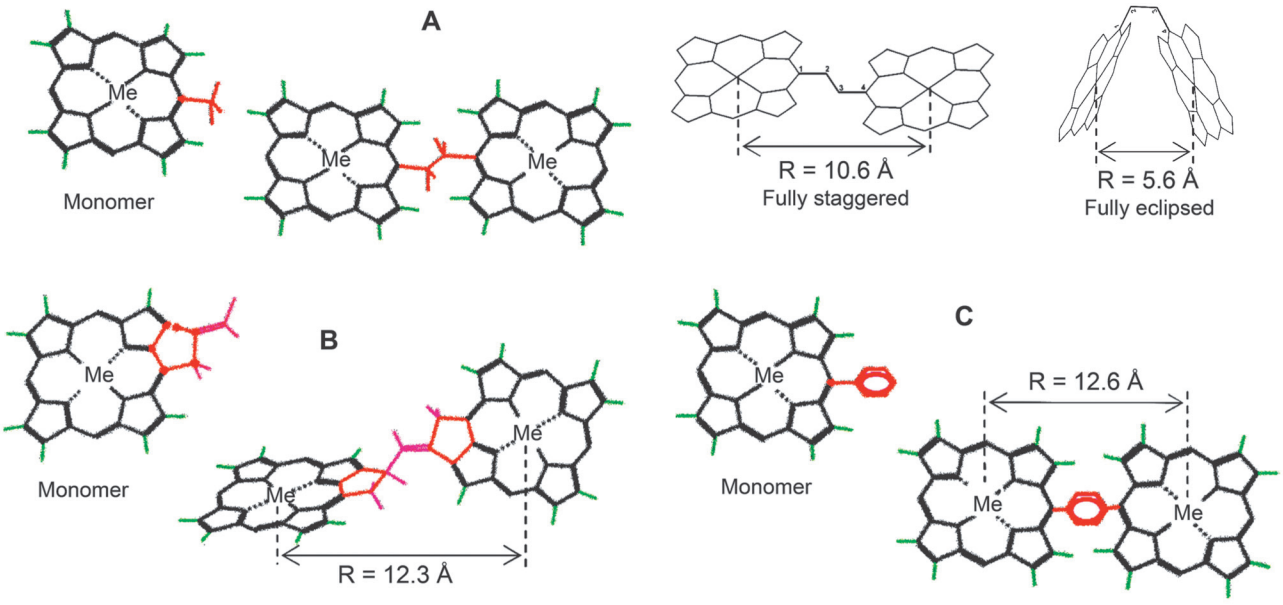

Figure 1. Chemical structures for a series of monomeric porphyrin precursors (Monomers) and their chemical dimers with various spacers between coupled π-conjugated macrocycles: A – ethane-bisporphyrins based on octaethylporphyrin molecules with a single -CH_2-CH_2- flexible bond via *meso*-positions.[62-67] Two conformations (fully eclipsed and fully staggered) with corresponding intercenter distances are shown. Temperature NMR ^{1}H studies have revealed that the fully staggered conformer has the lowest energy, that is presumably this conformer exists at 77 K while at 293 K a mixture of various conformers takes place. B – 3^1,5^{1}cyclodimers where one cyclopentaneporphyrin molecule (Me-OEP-cycle) is coupled with other cyclopentaneporphyrin molecule (Me-OEP-cycle=CH_2) via isocycles.[68-73] The planes of the Zn-3^1,5^1-cyclodimer subunits form an angle of approximately 78°. C – chemical dimers of octaethylporphyrins linked by a phenyl ring via *meso*-positions.[17,18,27,74-76] Me: H_2, Zn and/or Cu.

following we have studied interchromophoric interaction for hybrid porphyrin dimers of various structure having different spacers between coupled π-conjugated macrocycles. The structures of these dimers together with precursor monomers are shown in Figure 1 where the intercenter distances are shown also. Below we will discuss our findings together with those being obtained later in other groups.

Homodimers without Cu-porphyrins. The comparative analysis of photophysical parameters for compounds presented in Table 1 shows that interchromophoric interactions in homodimers with various spacers [ethane-bisporphyrins $(OEP)_2$ or $(ZnOEP)_2$, chemical dimers with phenyl spacer, $(OEP)_2Ph$ or $(ZnOEP)_2Ph$] do not alter essentially parameters of homodimer subunits relative to the corresponding monomeric compounds. The homodimer S_1state is deactivated mainly through intersystem crossing to T_1 state where the excitation is lost via non-radiative processes. Dipole-dipole interactions in these homodimers ($1.5\ cm^{-1} \le V_{12} \le 11\ cm^{-1}$) leads to the S-S Foerster resonance energy transfer (ET) between interacting subunits (rate constant $k_{EM}^{SS}=(0.15-13.5)\times10^{10}\ s^{-1}$). Essentially, this ET process takes place without quantum losses and is much faster than the other deactivation processes in homodimers ($k_{\Sigma}=(0.9-1.2)\times10^{8}\ s^{-1}$).[62-67] The same basic conclusions have been derived for homodimers with phenyl spacer, $(OEP)_2Ph$ or $(ZnOEP)_2Ph$.[17,74-76] As a result, at 293 K numerous "jumps" of excitation between the subunits within the S_1 state decay manifest themselves in the "collapse" of fluorescence excitation polarization spectra of homodimers compared to the corresponding individual monomers. In the case of Zn-cyclodimers (not presented in Table 1) ET can involve differently polarized S_0-S_1 and S_0-S_2 transitions of the dimer subunits, since they are close in energy scale.[69,73] It follows from data based on the donor fluorescence quenching and sensitization of acceptor emission that the quantum efficiency of ET $D \rightarrow A$ corresponds to $\Phi_{DA}=0.99$ at 293K and $\Phi_{DA}=0.95$ at 77 K, and also ET takes place without quantum losses in spite of a close proximity of interacting macrocycles. On the other hand for these dimers, the theoretical value Φ_{DA}^{theor} of quantum efficiency of ET $D \rightarrow A$ (calculated in frame of the Foerster model[42,43] using both computer-aided simulation of Zn-cyclodimer structures and experimental data on linear dichroism and fluorescence polarization) was found to be in a nice agreement with experimental findings.[69] It indicates that the Foerster theory of inductive resonance is still applicable to weakly interacting porphyrin π-conjugated macrocycles with the intercenter distance R≈10÷12.6 Å.

Heterodimers without Cu-porphyrins. Heterodimers containing a Cu ion in the center of one subunit have some general features.[62-70] In the case of the heterodimers $(H_2P+Cu)(OEP)_2$ and $(Zn+Cu)(OPP)_2$ the emission belongs to the H_2- or Zn-subunit, but is drastically quenched ($\varphi/\varphi_0 \approx 40$, Table 1). The singlet-singlet ET from Cu-subunit to H_2- or Zn-subunit having a S_0-S_1 transitions is not detected, and, additionally, the lifetime of the T_1 state (τ_T) of H_2- or Zn-subunits is decreased in these heterodimers compared to the corresponding homodimers without Cu-porphyrins. On the other hand, at 77 K phosphorescence of the Cu-subunit in $(H_2P+Cu)(OEP)_2$ and $(Zn+Cu)(OPP)_2$ is not detected due to the directed exchange coupled triplet-triplet ET to the H_2- or Zn-subunit ($k_{EM}^{TT} \ge 2\times10^{7}\ s^{-1}$). The same peculiarities were observed for the mixed dimers $(Cu+H_2)(OEP)_2Ph$ where two porphyrin molecules are coupled via meso-phenyl ring.[27,33,67,75] Scheme of excited states and main deactivation processes for heterodimers of these two types is shown in Figure 2.

Thus, keeping in mind exchange d-π effects known for monomeric Cu-porphyrins[52-58] and discussed in Introduction, one may conclude that in heterodimers with the intercenter distance R≈10÷12.6 Å the interaction of the unpaired

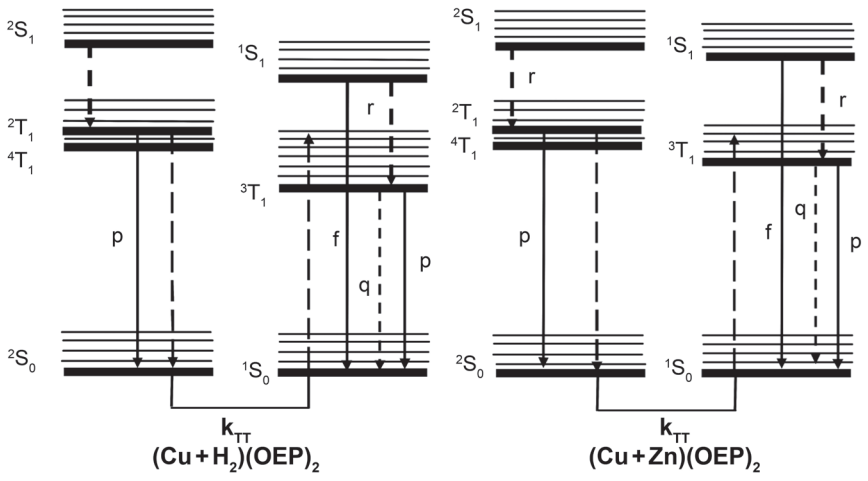

Figure 2. Schematic energy level diagram for low-lying locally excited singlet and triplet states of interacting counterparts in hybrid dimers $(Cu+H_2)(OEP)_2$ and $(Cu+Zn)(OEP)_2$ with different ($-CH_2-CH_2-$ or phenyl) spacers. Indicated are rate constants of the following pathways: f, fluorescence decay $^1S_1 \rightarrow {}^1S_0$; r, intersystem crossing $^1S_1 \sim\sim> {}^3T_1$ ($^2S_1 \sim\sim> {}^2T_1$ in the case of Cu-containing components); p, phosphorescence decay $^3T_1 \rightarrow {}^1S_0$ ($^2T_1 \rightarrow {}^2S_0$ in the case of Cu-containing components); q, k_{TT}, triplet-triplet energy transfer from thermally equilibrated "trip-doublet" ($^2T_1$) and "trip-quartet" ($^4T_1$) states of Cu-porphyrin half to the locally excited T_1 states of porphyrin free base or Zn-porphyrin halves. For simplicity, intrinsic non-radiative decays of "trip-doublet" ($^2T_1$) and "trip-quartet" ($^4T_1$) states of Cu-porphyrin halves are not shown.

Table 1. Excited state parameters for porphyrin chemical dimers and their precursor monomeric subunits.

Compound	φ_F [a] 295 K	φ_F 77 K	τ_S [a] (ns) 295 K	τ_S (ns) 77 K	τ_T [a] (μs) 295 K	τ_T (μs) 77 K	τ_P (μs) 77 K	φ_P 77 K	λ_P (nm) 77 K
		Precursor	Monomers with corresponding side *meso*-substituents						
OEP-*meso*CH_3	0.03[d]	0.04[d]	10.7[d]	15.5[d]	1000	7600[d]	8600	0.0002	794
OEP-*meso*Ph	0.05	0.09	16.0	21.0	4.0[e]	11100	13500	0.0002	790
ZnOEP-*meso*CH_3	0.015[d]	0.02[d]	1.7[d]	2.3[d]	1200	31400[d]	35000	0.007	745
ZnOEP-*meso*Ph	0.02	0.03	1.6	2.3	5.8[e]	32000	39000	0.03	706
CuOEP	–	–	–	–	0.120[f]	65	72	0.14	680
CuOEP-*meso*CH_3	–	–	–	–	0.025[b]	160[d]	150	0.04	690
CuOEP-*meso*Ph	–	–	–	–	0.025[b]	40	48	0.05	684
			Ethane-bisporphyrins with -CH_2-CH_2- spacer						
$(OPP)_2$[c]	0.025[d]	0.035[d]	8.2[d]	11.6[d]	1100	6300[d]	7600	0.00002	830
$(ZnOPP)_2$[c]	0.02[d]	0.03[d]	1.5[d]	2.3[d]	1150	33900[d]	41000	0.015	764
$(CuOPP)_2$[c]	–	–	–	–	0.25[b]	130	80	0.02	717
$(Cu+H_2)(OEP)_2$	0.0013	0.0018	–	–	0.9	350[d]	300	0.003	842
$(Cu+Zn)(OEP)_2$	0.0002	0.0004	–	–	0.7	7900/1100[d]	9200/1900	0.04	760
			Chemical dimers with the phenyl spacer						
$(OEP)_2$Ph	0.06	0.08	11.2	16.0	2.45[e]	3900	7600	0.00003	810
$(ZnOEP)_2$Ph	0.015	0.025	1.2	2.1	2,85[e]	27000	38000	0.01	740
$(CuOEP)_2$Ph	–	–	–	–	0.015[b]	0.28	0.24	0.01	762
$(Cu+H_2)(OEP)_2$Ph	0.002	0.0025	–	–	0.035[b]	108	100	0.008	830
			Cyclopentaneporphyrins and the dimer with the covalent link via isocycles						
OEP-cycle	0.05	0.10	16.0	22.4	–	19500	–	–	–
OEP-cycle=CH_2	0.04	0.09	15.0	21.1	–	23000	–	–	–
ZnOEP-cycle	0.015	0.02	1.9	2.9	–	72500	–	–	–
ZnOEP-cycle=CH_2	0.025	0.05	1.8	3.5	–	44500	–	–	–
CuOEP-cycle	–	–	–	–	–	160	180	0.13	680
CuOEP-cycle=CH_2	–	–	–	–	–	220	200	0.02	689
$3^1,5^1$-cyclodimer	0.04	0.10	15.0	22.5	–	21600	–	–	–
Zn-$3^1,5^1$-cyclodimer	0.03	0.04	1.8	3.0	–	57400	–	–	–
Cu-$3^1,3^1$-cyclodimer	–	–	–	–	–	170	190	0.02	693

Notes: φ_F and τ_S are fluorescence quantum yield and lifetime values; τ_T and τ_P are excited triplet state decays measured by pump-probe and kinetic phosphorescence methods, correspondingly; φ_P is phosphorescence quantum yield; λ_P values were measured at maxima of the shortest phosphorescence bands. In the case of Cu-containing monomers and symmetrical dimers, the fluorescence was not observed within the limits of the experimental setup sensitivity ($\varphi_F<10^{-5}$) in the temperature range of 77-295 K.

[a]At 295 K these values were measured for degassed solutions (TOL or MCH), at 77 K rigid glassy matrices (MCH, solvent mixture EPIP) were used.

[b]Obtained by the deconvolution procedure with accuracy of ±30% taking into account the experimental response of the pump-probe setup.

[c]The comparison of octapropyl- (OPP) and octaethylporphyrin (OEP) derivatives seems to be reasonable as far as all spectral and energetic parameters for these compounds coincide practically.[70]

[d]Given from our previous paper.[63]

[e]Given from our previous papers.[75, 76] As a rule, pump-probe and kinetic phosphorescence measurement have shown that the corresponding decays are multiexponential. For τ_T and τ_P values presented data reflect the monoexponential fit.

d-electron of central Cu ion of Cu-porphyrin subunit with π-conjugated system of the other half leads to an increase of the intersystem crossing rate constant in the last one. As a result, the lifetimes of S_1 and T_1 states in the H_2- and Zn-subunits of the heterodimers are reduced compared to those for the corresponding homodimers.

At present, taking into account the discussed results and those of other groups being obtained later, the specificity of the electronic excitation energy relaxation in Cu-porphyrin containing hybrid dimers may be considered as follows. For (H_2P+CuP) or (ZnP+CuP) pairs the non-radiative singlet-singlet energy transfer from the energetically higher paramagnetic Cu ion containing half has not been detected,[63,70,102-107] that is explained by rapid intersystem crossing in the copper porphyrin moiety. In the case of (H_2P+CuP) dimers, ET process occurs from thermally

equilibrated "trip-doublet" ($^2T_1$) and "trip-quartet" ($^4T_1$) states of Cu-porphyrin half to the locally excited T_1 state of porphyrin free base half, that has been detected by steady-state as well as μs-ns time-resolved phosphorescence and T-T absorption measurements,[63,70,106-110] time-resolved EPR spectroscopy.[110-114] In the result, at 77 K the energy transfer of this type (being exchange resonant by nature[44] manifests itself in the strong decrease of quantum yield of CuP moiety phosphorescence and the appearance of H_2P sensitized phosphorescence as well as the weakening of T-T transient absorption intensities for copper containing half accompanied by the strengthening of the amplitude of T-T transient absorption belonging to porphyrin free base half of the hybrid dimer.[63,70,109] In addition, the intramolecular T-T ET in hybrid (H_2P+CuP) dimers with flexible spacer has been proven by time-resolved ESR study at 77 K showing that spin polarization of the free base moiety in the hybrid dimer differs from that for the free base porphyrin monomer.[112] At last, it should be mentioned that for hybrid (H_2P+CuP), the realization of the effective T-T energy transfer with the rate constant $k_{TT} > 6\times10^7$ s^{-1} seems to be the only one reason leading to the increase of the quantum yield of singlet oxygen generation by such dimers compared to that found for homo-ethane-bisporphyrins (H_2P+H_2P) in liquid solutions at room temperature.[27,34,115] Obviously, the efficiency of the intramolecular T-T energy transfer in covalently linked systems depends on the electronic interactions between two components. In the case of (H_2P+CuP) or (ZnP+CuP) hybrid dimers, two possible ways of electronic communications may be realized: 1) the direct overlap of the donor and acceptor molecular orbitals,[63,70] especially enhanced for the dimers with flexible spacers;[106-108,112,13] 2) superexchange interactions depending on the electronic properties of the bridge (spacer).[109,114,116]

The existence of a Cu-containing porphyrin in (H_2P+CuP) or (ZnP+CuP) hybrid dimers with a relatively close proximity of interacting halves manifests itself in the increase of the non-radiative deactivation of S_1 states for the dimer half not containing central Cu ion.[63,70,109,114] The fluorescence lifetime shortening and quantum yield decrease being detected for Zn- or free base porphyrin counterparts are caused mostly by the enhancement of the intersystem crossing in these halves. This enhancement is explained by the existence of the exchange coupling of unpaired d-electron of central Cu(II) ion of one half of the dimer with π-conjugated electronic system of the other half.[63,102,103,109] For some hybrid dimers this coupling may be governed by through-bond interactions via spacer.[114] Moreover, for hybrid (ZnP+CuP) dimers with *meso* -CH_2-CH_2- spacer the thermally activated singlet-singlet energy transfer from Zn-porphyrin to Cu-porphyrin has been observed at room temperature being the additional reason of fluorescence quenching for Zn-porphyrin component.[63]

In its turn, the existence of the exchange d-π coupling in (H_2P+CuP) or (ZnP+CuP) hybrid dimers leads also to the strengthening of the non-radiative T_1~~>S_0 transitions in

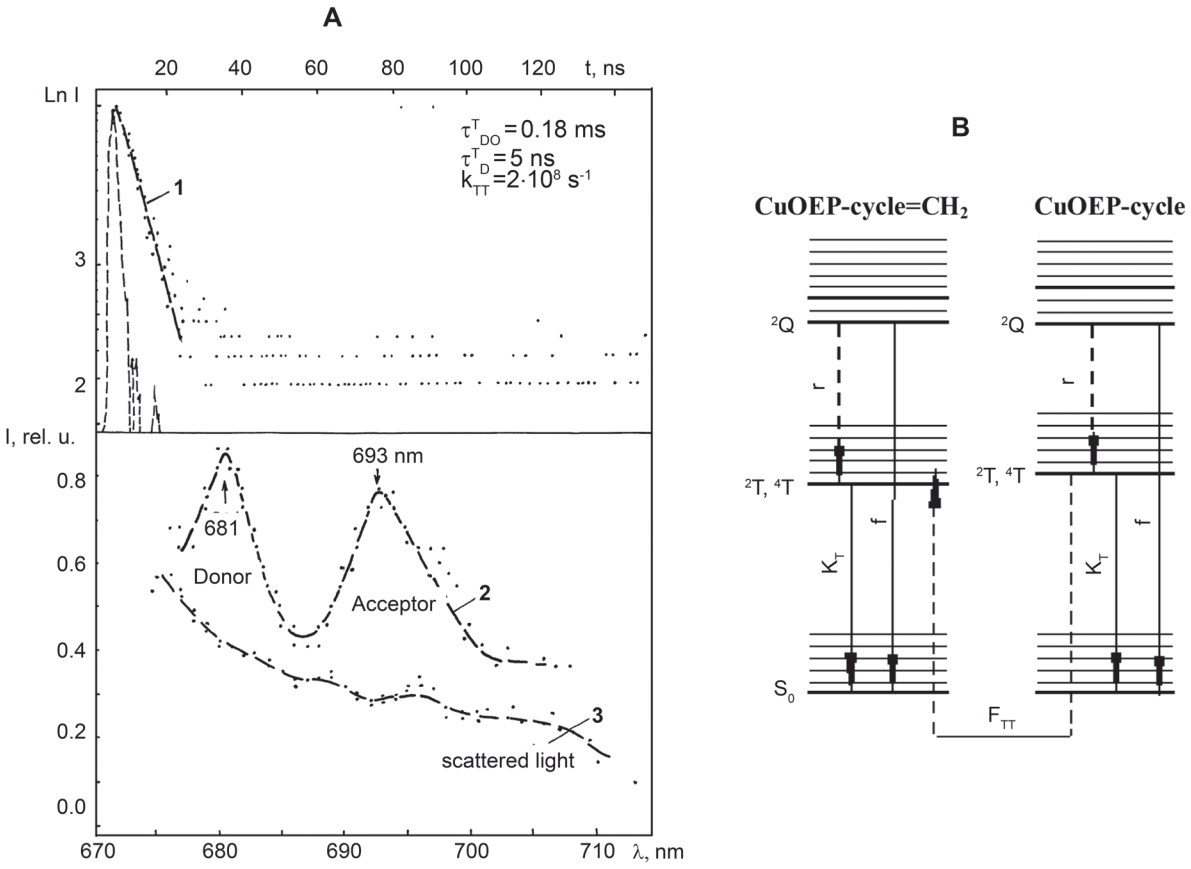

Figure 3. A: Phosphorescence decay trace (1, λ_{exc} = 380 nm, λ_{reg} = 680 nm), phosphorescence spectrum at delay time θ = 3.8 ns (2, $t_{1/2}$ = 2.5 ns, Δθ = 25 ns) for Cu-cyclodimer in tetrahydrofurane-toluene mixture (3:1) at 77 K. B: Energy levels scheme and directionality of the energy transfer for Cu-cyclodimer in these conditions.

Zn- or free base porphyrin counterparts. Really, the strong shortening of T_1 state decays has been observed for these halves in hybrid dimers at room temperature[107,108] and 77 K.[63,112] In some papers[110,117] the additional quenching of locally excited states in (ZnP+CuP) hybrid dimers is discussed to be connected with the formation of short-lived radical ion pair formed by the photoinduced electron transfer from the excited singlet precursor.

Finally, in the case of Cu-cyclodimers, fast intersystem crossing to the ^{2,4}T states with rate constant $k=3\times10^{13}$ s^{-1} in both subunits containing central Cu ion (structure B in Figure 1) prevents the singlet-singlet energy transfer between donor and acceptor (theoretical rate constant is of $k_{ET}^{theor}<4\times10^{10}$ s^{-1}). Nevertheless, a strong quenching of the donor (CuOEP-cycle) phosphorescence is observed for these dimers at 77 K.[72] Moreover, in phosphorescence excitation spectra of the acceptor (CuOEP-cycle=CH_2) new bands belonging to the donor absorption have been observed. These results evidently show that the phosphorescence quenching of the donor in Cu-cyclodimers is due to an exchange ET via T-levels of interacting subunits at the intercenter distance R≈12.3Å. The real manifestation of such a process is proven also upon detection of phosphorescence spectra for Cu-cyclodimer at 77 K at various delay times after the laser pulse, where rate constant of ($k_{TT}=2\times10^8$ s^{-1}) from CuOEP-cycle to CuOEP-cycle=CH_2 has been evaluated directly (see Figure 3).

In the frame of Dexter model[44] for exchange resonance interactions (when absorption transition of acceptor is forbidden) the rate constant of T-T energy transfer is calculated as follows:

$$k_{TT}^{exch} = \left(4\pi^2/h\right)\cdot Z\cdot\exp\left(-2R/L\right)\frac{\int f_D(\nu)\varepsilon_A(\nu)d\nu}{\int f_D(\nu)d\nu\cdot\int\varepsilon_A(\nu)d\nu}, \quad (3)$$

where L is mean effective van der Waals radius for initial and final states of D and A molecules (considering spatial overlap of molecular orbitals for interacting counterparts), Z – is constant with the energy dimensionality (which is not connected with any experimental value), the rest factor is the normalized overlap integral calculated for emission spectrum of the donor and absorption spectrum of the acceptor. Based on ideas discussed in[102] and theoretical calculations of the normalized overlap integrals for the dimers under consideration[87] the estimated values for T-T energy transfer for Cu-cyclodimer should be $k_{TT}^{theor}\approx7\times10^7$ s^{-1} thus being in an appropriate agreement

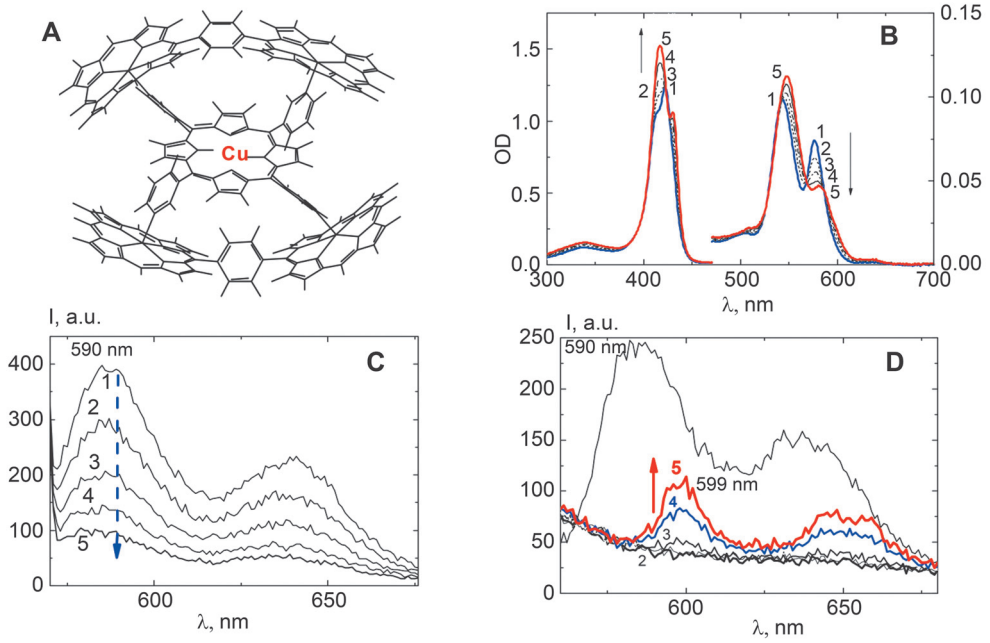

Figure 4. Formation and spectral properties of pentad 2(ZnOEP)$_2$Ph⊗CuP(mPyr)$_4$ in toluene. **A**: Mutual arrangement of the dimer (ZnOEP)$_2$Ph and extra-ligand CuP(mPyr)$_4$. For clarity, β-ethyl substituents in (ZnOEP)$_2$Ph are omitted. (HyperChem software, release 4.0 geometry optimization with semiempirical PM3 method). The symbol ⊗ is used in order to show what interacting subunits (dimer and extra-ligands) are bound together.
Absorption (**B**) and fluorescence (**C**) spectra of the dimer (ZnOEP)$_2$Ph upon titration by extra-ligand CuP(mPyr)$_4$, in toluene at 293 K and temperature dependence of the pentad 2(ZnOEP)$_2$Ph⊗CuP(mPyr)$_4$ emission spectra upon temperature lowering (**D**).
A: Absorption spectra transformations at various molar ratio x=[CuP(mPyr)$_4$]/[(ZnOEP)$_2$Ph)]: 0.14 (1), 0.29 (2), 0.43 (3), 0.57 (4), and 0.71 (5).
B: Fluorescence intensity decrease (λ_{ex}=567 nm, isosbestic point) of the uncomplexed dimer (λ_{max}=590-591 nm) upon the sequential increase of molar ratio x: 0.14 (1), 0.29 (2), 0.43 (3), 0.57 (4), and 0.71 (5). At x=0.71 the rest of the non-red shifted fluorescence belongs to non-complexed dimer.
C: Fluorescence spectra (λ_{ex}=542 nm) of the pentad 2(ZnOEP)$_2$Ph⊗CuP(mPyr)$_4$ (x=0.71) in toluene (thin transparent layers) at various temperatures: 300 K (1, belongs to the rest of the non-complexed dimer), 220 K (2, additional quenching is due to the full complexation), 190 K (3), 165 K (4), and 150 K (5). The red-shifted fluorescence bands at T≤210 K (increasing upon temperature lowering) belong to the emission of the dimer extra-ligated by CuP(mPyr)$_4$ in pentad. Adopted from. [80]

with experimentally determined value $k_{TT}^{exper}=2\times10^8$ s^{-1}. In this case, the experimental value of the T-T transfer rate constant is much higher than the rate constant of the donor T-state deactivation ($k^0_T=6.7\times10^3$ s^{-1}). Interestingly, the rate constant k_{TT} of exchange T-T energy transfer is close to the values of rate constants characteristic for deactivation of S_1 level in H_2-cyclodimers ($k_S=(4\text{-}5)\times10^7$ s^{-1}). Taking into account this fact it is not excluded that an exchange S-S EM may be responsible for the additional quenching of the donor fluorescence in the H_2-cyclodimers of the same structure where the dipole-dipole interactions are weak compared to those in the corresponding Zn-complexes.

Multiporphyrin Self-Assembled Complexes with Cu-Porphyrin Subunit

Keeping in mind the specificity of interchromophoric interactions in Cu-porphyrin containing hybrid chemical dimers (discussed in previous section) we found that long-distant exchange d-π effects manifest themselves also in more complex multiporphyrin self-assembled arrays such as pentads and larger complexes[38,118] with well-defined geometry and containing Cu-porphyrin subunit. Two examples of the observed finding are the following.

In toluene at ambient temperature, titration of the homodimer $(ZnOEP)_2Ph$ by tetra-*meta*-pyridyl containing molecules leads to the formation of pentads $2(ZnOEP)_2Ph\otimes CuP(mPyr)_4$ containing two dimers bonded to the extra-ligand $CuP(mPyr)_4$ via non-covalent binding interactions[77-80] (Figure 4A). Almost the same spectral position of the Soret band components and practically doubled extinction coefficients of the pentad compared to those of the triads[74] lead to the conclusion that the intense B-transitions of two dimers $(ZnOEP)_2Ph$ bound in the same pentad are not involved into strong coupling. Like in the case for other pentads of the same geometry[38,77,80,118] the formation of the pentad $2(ZnOEP)_2Ph\otimes CuP(mPyr)_4$ are characterized by a slight red shift of the dimer and ligand visible electronic bands which is larger with respect to that for the corresponding triads.[74] This shift and differences may be explained by a larger distortion of tetrapyridyl-containing extra-ligands from planarity in the pentad relative to that for dipyridyl-containing porphyrins in the triad. Figure 4B shows that the dimer fluorescence is strongly quenched in the pentad $2(ZnOEP)_2Ph\otimes CuP\text{-}(m\text{-}Pyr)_4$. Noteworthy, at x=0.71 the rest of the non-red-shifted fluorescence belongs to non-complexed dimer $(ZnOEP)_2Ph$ exclusively.

Taking into account spectral-kinetic parameters as well as redox properties of interacting subunits in the pentad $2(ZnOEP)_2Ph\otimes CuP(mPyr)_4$ several processes may influence on the dimer fluorescence in this complex (Figure 5): i) the photoinduced electron transfer (PET) Zn-dimer*…CuP]→[Zn-dimer$^+$…CuP$^-$]; ii) thermally activated ET from the dimer S_1 state to ^2Q state of $CuP(mPyr)_4$ at the intercenter distance R_{DA}=8.8 Å; iii) exchange d-π effects leading to an increase of the intersystem crossing rate constant in the dimer subunits caused by an interaction of Cu unpaired d-electron with π-conjugated systems of the dimers.

With respect to the given pentad, the corresponding analysis gives the following. According to Marcus theory,[46,47] adiabatic PET in a "normal" region becomes possible if the Gibbs free energy of the process $\Delta G^0<0$. With respect to the pentad, Gibbs free energy of PET reaction may be calculated according to:[119]

$$\Delta G^0=e(E_D^{OX}-E_A^{RED})+\Delta G_S-E(S_1^D). \quad (4)$$

The oxidation potential for coordinated dimer $(ZnOEP)_2Ph$ was taken to be E_D^{OX}=0.63 V, like for pyridinated ZnOEP in dimethylforamide (DMF) *vs*. SCE.[120] Reduction potential for $CuP(mPyr)_4$ $E_A^{RED}=-1.07$ V (in DMF *vs*. SCE) has been extracted from literature data taking into account that pyridyl substituents increase the reduction potential of tetrapyrrolic macrocycles.[80,119] Correction term for the position of CT state in toluene at 293 K was

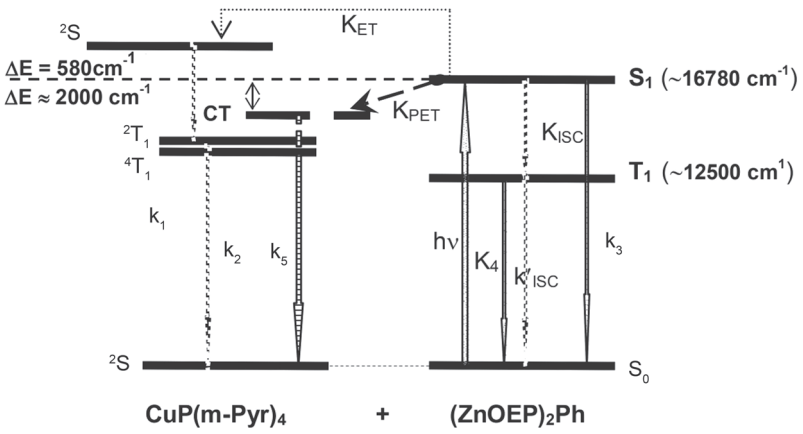

Figure 5. Schematic energy level diagram of excited states for pentad $2(ZnOEP)_2Ph\otimes CuP(mPyr)_4$. Indicated are rate constants of the following pathways: k_1, fluorescence and non-radiative decay of the dimer or extra-ligand; k_{ISC}, intersystem crossing S_1~~>T_1; k_2, radiative and non-radiative decay of Cu-porphyrin triplet state; k_{ET}, thermally activated ET dimer→extra-ligand; k_{TT}, T-T exchange ET from Cu-porphyrin→dimer; k_{PET}, photoinduced electron transfer leading to the radical ion pair $[(ZnOEP)_2Ph^+…CuP^-]$ formation. ΔE is the energy gap between excited singlet states of the corresponding subunits.

calculated to be ΔG_S=0.287 eV, with donor and acceptor radii of r_D=r_A=5.5 Å and intercenter distance of R_{DA}=8.8 Å for the pentad optimized structure.[80,119] Thus, in toluene at ambient temperature $E(IP)=e(E_D^{OX}-E_A^{RED})+\Delta G_S$=1.99 eV, ΔG^0=–0.14 eV<0, and PET at R_{DA}=8.8 Å might become rather effective and fast (within tens of picoseconds) in the given complex.

At ambient temperature (kT=209 cm^{-1}) thermally activated inductive-resonance ET from the dimer S_1 state to ^{2}Q state of CuP(mPyr)$_4$ (energy gap ΔE≈580 cm^{-1}, see Figure 5) is still possible with the rate constant k_{ET}^{theor} ≤3.7·10^9 s^{-1}.[80] Thus, like for hybrid (ZnP+CuP) dimers (discussed above), this process in the pentad may lead to the additional fluorescence quenching of both dimers (ZnOEP)$_2$P in the pentad.

In order to discriminate these processes we did the following. Obviously, temperature lowering and transition to rigid solutions would lead to the switching off two processes in the pentad 2(ZnOEP)$_2$Ph⊗CuP(mPyr)$_4$: i) thermally activated ET (ZnOEP)$_2$Ph⊗CuP(mPyr) due to Boltzmann factor exp(-ΔE/kT) increase and the decrease of spectral overlap integral (thus both leading to the overall k_{ET} diminishing), and ii) photoinduced electron transfer due to the destabilization of the ion pair [Zn-dimer$^+$…CuP$^-$] state.[121] In contrast, exchange d-π effects are hardly dependent on temperature.[52-59,62,63,108-112] Experimental findings presented in Figure 5D show that upon temperature lowering from 293 K down to T≈210 K an additional quenching of the non-complexed dimer is still observed caused by the full complexation at low T. At the same time, fluorescence of the complexed dimer (ZnOEP)$_2$Ph in the pentad 2(ZnOEP)$_2$Ph⊗CuP-(m-Pyr)$_4$ remains still strongly quenched like that found at 293 K. The most interesting observation is that upon further temperature lowering (down to 190 K (curve 3), 165 K and 150 K (curve 4), a small pronounced increase of the red-shifted fluorescence band belonging to the dimeric subunit in the pentad (like di-pyridinated homodimer (ZnOEP)$_2$Ph[74,80]) is evidently seen. It means that in a temperature range of 150÷293 K the emission strong quenching for both dimers (ZnOEP)$_2$Ph in the pentads containing CuP(mPyr)$_4$ extra-ligand, is caused by exchanged d-π effects presumably which remain still pronounced even at intercenter distances R_{DA}=8.8 Å.

Following these conclusions made for pentads we prepared larger multipotrphyrin complexes using chemical trimer (ZnOEP)$_3$Ph$_2$ and the same self-assembly approach with two extra-ligands H$_2$P(m-Pyr)$_4$ and CuP(m-Pyr)$_4$ in toluene at 295 K (Figure 6A). At the first intermediate stage,

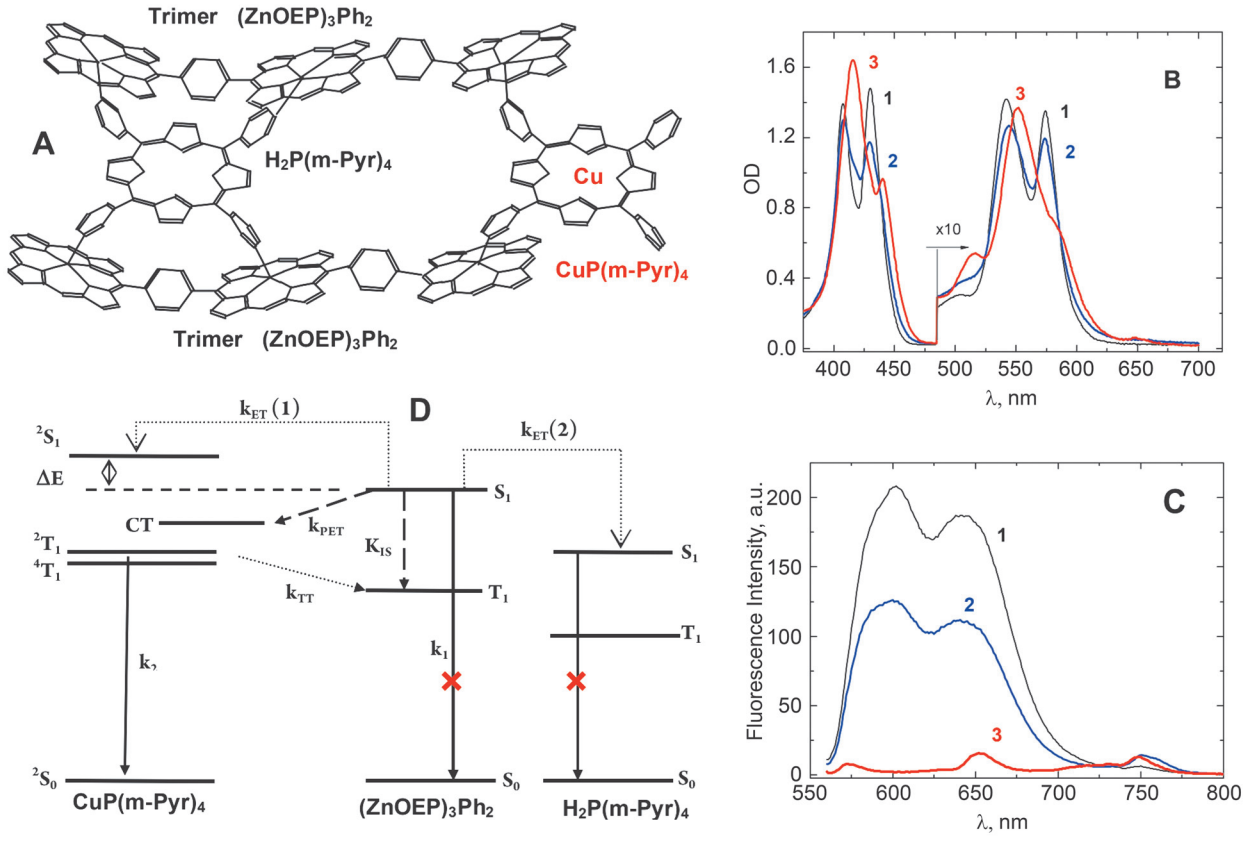

Figure 6. Formation and spectral properties of self-assembled complexes with participation of the trimer (ZnOEP)$_3$Ph$_2$ and two extra-ligands H$_2$P(m-Pyr)$_4$ and CuP(m-Pyr)$_4$ in toluene at 295 K. **A**: Mutual arrangement of the trimer and extra-ligands in the complex 2(ZnOEP)$_3$Ph$_2$⊗H$_2$P(m-Pyr)$_4$⊗CuP(mPyr)$_4$. For clarity, β-ethyl substituents in the trimer (ZnOEP)$_3$Ph$_2$ are omitted. Absorption (**B**) and fluorescence (**C**, λ_{ex}=570 nm) spectra of the toluene solution with the trimer (ZnOEP)$_3$Ph$_2$ upon sequential one-step addition of two extra-ligands H$_2$P(m-Pyr)$_4$ and CuP(m-Pyr)$_4$. **C**: emission spectra of pure trimer (ZnOEP)$_3$Ph$_2$ (1), intermediate mixture (ZnOEP)$_3$Ph$_2$+H$_2$P(m-Pyr)$_4$ (2:1) and final mixture (ZnOEP)$_3$Ph$_2$+ H$_2$P(m-Pyr)$_4$ + CuP(m-Pyr)$_4$ (2:1:1). **D**: Schematic energy level diagram of excited states for the complex 2(ZnOEP)$_3$Ph$_2$⊗H$_2$P(m-Pyr)$_4$⊗CuP(mPyr)$_4$. Rate constants are described in Figure 5.

the complex $2(ZnOEP)_3Ph_2 \otimes H_2P(m\text{-}Pyr)_4$ has been formed by one-step titration (see spectra 2 in Figure 6B and 6C). As predicted, at ambient temperature fluorescence of the trimer is quenched (like in triads and pentads with the dimer $(ZnOEP)_2Ph$ and $H_2P(m\text{-}Pyr)_n$ extra-ligands[21,27,78,80]) due to competitive processes: singlet-singlet ET trimer$\rightarrow H_2P(m\text{-}Pyr)_4$ and charge transfer (^{1}Trimer*...Lig)$\rightarrow$(Trimer$^+$...Lig$^-$). The emission of the extra-ligand is also noticeably quenched via two charge transfer processes leading to the non-radiative deactivation of the locally excited S_1 states of the ligand in nano-, picosecond time scale [(^{1}Dimer*...Lig)$\rightarrow$(Dimer$^+$... Lig$^-$), (Dimer...^{1}Lig*)$\rightarrow$(Dimer$^+$...Lig$^-$)].[21,27,78,80,83,84] At the next stage, the other extra-ligand $CuP(m\text{-}Pyr)_4$ has been added in one step to the solution thus having the final mixture $(ZnOEP)_3Ph_2 + H_2P(m\text{-}Pyr)_4 + CuP(m\text{-}Pyr)_4$ (2:1:1) (see spectra 3 in Figure 6B and 6C).

Importantly, the existence of $CuP(mPyr)_4$ in the complex $2(ZnOEP)_3Ph_2 \otimes H_2P(m\text{-}Pyr)_4 \otimes CuP(mPyr)_4$ manifests itself in the observable fluorescence quenching for both $(ZnOEP)_3Ph_2$ and $H_2P(m\text{-}Pyr)_4$ subunits like it has been observed also for such complexes of different morphology and composition.[38,80,118] The basic explanation of this additional quenching is in the scope of our findings discussed above. Really, it follows from the energetic scheme (Figure 6D) for the complex $2(ZnOEP)_3Ph_2 \otimes H_2P(m\text{-}Pyr)_4 \otimes CuP(mPyr)_4$ that the photoinduced electron transfer $H_2P(m\text{^}Pyr)_2 \rightarrow CuP(mPyr)_4$ is impossible due to thermodynamic reasons ($\Delta G^0>0$). On the other hand, the dipole-dipole energy transfer $H_2P(m\text{-}Pyr)_4 \rightarrow CuP(mPyr)_4$ is low probable due to a high energy gap $\Delta E \approx 1950$ cm^{-1} at ambient temperature. Thus, the only adjustable reason responsible for the fluorescence quenching of both $(ZnOEP)_3Ph_2$ and $H_2P(m\text{-}Pyr)_4$ subunits in the complex with $CuP(mPyr)_4$ is the enhancement of the non-radiative intersystem crossing in these subunits due to exchange d-π effects caused by relatively distant Cu atom of attached $CuP(mPyr)_4$ ligand.

Ordered Aggregates of Photosynthetic Pigments with Admixture of Cu-Pheophytin Molecules

Polymeric ordered aggregates of chlorophyll *a* (Chl *a*) and protochlorophyll *a* (PChl *a*) have been prepared and studied at low initial concentrations of the pigments (1×10^{-5} M) in binary mixture of water and dioxane (4:1).[85-88] The two oxygen atoms of the dioxane molecule are able to link two Chl *a* (or PChl *a*) molecules by coordinating to the central magnesium atoms of the tetrapyrrolic macrocycles with center-to-center distance R≈7 Å (Figures 7A and 7D). Due to the molecular structure of dioxane, other types of bonding are not possible. The low concentration of chlorophylls in sample preparations supports the view that the dynamic energy transfer between individual aggregates of these type in solution is inadequate to explain the characteristics observed for the Chl *a*-dioxane (or PChl *a*) aggregates. Absorption and fluorescence spectra of the aggregates (1 and 2 in Figure 7C) are red-shifted (by ≈20 nm) with respect to those for the corresponding monomers. Main structural and photophysical properties of individual aggregates are as follows.

To study the relationship between the structure and spectral properties of the aggregates, several one-dimensional model structures of Chl *a*-dioxane aggregates were computed by the molecular mechanics method. Three overall structures ranging from stick to a ring shape were energetically favored for threes polymeric ordered aggregates (Figure 7B). All these structures contain structural heterogeneity that consists of repeating dimers that further form tetramer substructures. The detection of highly polarized fluorescence for these aggregates in water-

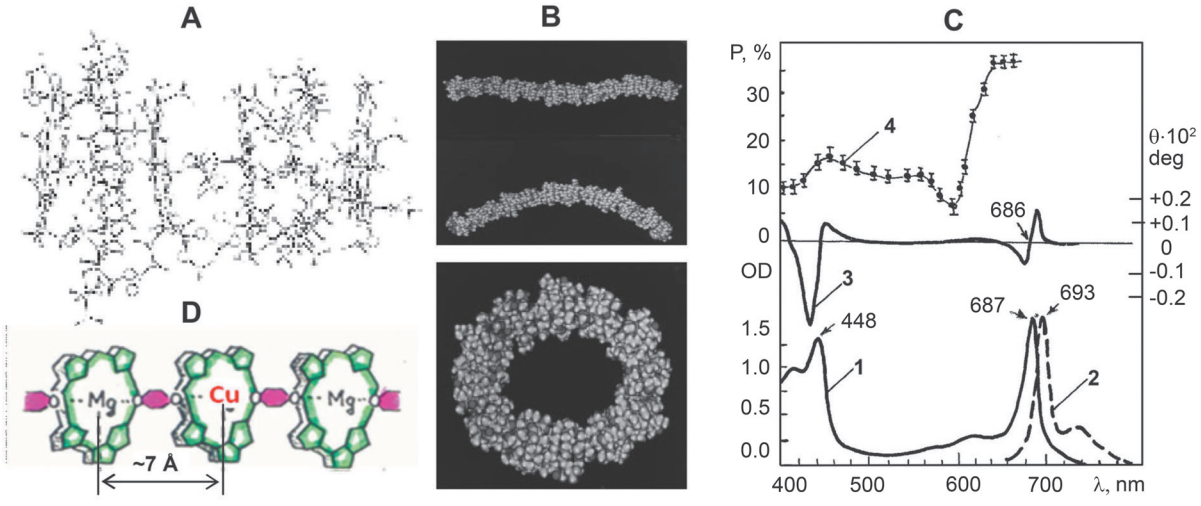

Figure 7. Structural organization of ordered aggregates of photosynthetic pigments (chlorophyll *a* or protochlorophyll *a*) and their spectral parameters in binary mixture of solvents (water-dioxane 4:1) at ambient temperature. **A**: Optimized structure of repeating tetramers of the Chl *a*-dioxane aggregate. **B**: Computed minimum energy structures of (Chl *a*-dioxane)$_{24}$ aggregates (stick, arc, and ring). Optimized structures were minimized by using a molecular mechanics method with the CHARMm force field and Newton Raphson optimization (adopted from[89]). **C**: absorption (1), fluorescence (2), circular dichroism (3) and fluorescence polarization spectra (4, λ_{det}=693 nm) of chlorophyll *a* aggregate. **D**: Part of the proposed structure of mixed aggregate of chlorophyll- or protochlorophyll *a* - Cu-pheophytin *a* (100:1) based on the experimental data.[85,87]

dioxane solutions at 293 K (4 in Figure 7C) reflects the high ordering of interacting π-conjugated macrocycles in these arrays. The circular dichroism (CD) signal (3 in Figure 7C) is strong (by two order of magnitude with respect to that for monomers[85-88]) and the sign sequence follows that of the polarization spectrum. ψ-Type effect in CD spectra (splitting into two components of the opposite sign) of these aggregates reflects the long-range interactions within the sizable aggregate frame. Thus, the non-radiative singlet–singlet ET can take place and the excitation can move from one elementary cell to another, which is demonstrated by the absence of fluorescence anisotropy in the SPC measurements and the independence of the fluorescence excitation spectra on the recording wavelength.[88] Additionally, the existence of the delocalized excitation is indicated also by the short lifetime observed for fluorescence emission of Chl *a*-dioxane aggregates (τ~40 – 90 ps), and the absence of the temperature effect on the fluorescence lifetimes indicates the excitation delocalization length to be not large enough.[88]

According to experimental results (analysis of the splitting in CD spectra of [87,88]) and quantum chemical calculations[89] excitonic (dipole-dipole) coupling in the dimeric cell of the PChl *a*-dioxane and Chl *a*-dioxane aggregates is estimated to be V_{12}~40 – 70 cm^{-1}. In this case, ET may be considered as non-coherent "hot" transfer with participation of non-relaxed states of interacting molecules in the aggregate where the dynamic correlation between donor and acceptor is absent.[122] Correspondingly, such "hot" transfer (Hot ET) takes place like localized exciton over the whole aggregate. Localization of excitation may be induced by the energy disorder of the aggregate, deep non-radiative trap or other reasons.

With this basic background, here we comparatively analyze the fluorescence quenching of PChl *a* in mixed PChl *a*-dioxane aggregates containing the increasing admixture of other molecules, such as Chl *a*, Pd-pheophytin *a* (Pd-Pheo) and Cu-pheophytin *a* (Cu-Pheo) presented in Figure 8.

Data presented in Figure 8 show that upon increase of the molar concentration of Chl *a*, Pd-Pheo and Cu-Pheo (C_A) the fluorescence quenching of PChl *a* matrix is strengthening being the most pronounced for Cu-Pheo (curve 3). It should be noted that the observed quenching effects are realized in mixed aggregates namely as far as the chromophore concentrations (C_0=1×10^{-5} M and C_A=10^{-8} – 10^{-5} M) are low enough to prevent a noticeable dynamic energy transfer between the individual aggregate units within pico-nanosecond time scale. On the other hand, the back ET from Chl *a*, Pd-Pheo and Cu-Pheo to PChl *a* is low probable also from the energetic and kinetic backgrounds. According to the Hot ET model[122] the localized exciton migration in PChl *a* aggregate takes place within t_{HM}~10-20 ps with pair jump of t_{PM} ~1-6 ps, and is characterized by the radius of the non-coherent hot migration R_{HM}~180 Å.[87] Taking this estimations, one may conclude that the main reason of PChl *a* fluorescence quenching in mixed aggregates PChl *a* – Chl *a* is the energy trapping of the localized exciton by Chl *a* admixture molecules. In the case of mixed aggregates PChl *a* – Pd-Pheo the main reason of the quenching may be explained by the perturbation action of heavy atom effect[59] in Pd-Pheo leading to the formation of exciton traps in the vicinity of this admixture in PChl *a* matrix.

Finally, the strongest quenching of PChl *a* matrix being observed in mixed aggregates with Cu-Pheo (especially at molar ratios PChl:Cu-Pheo=1000÷100) is definitely connected with exchange d-π effects influence on the neighboring PChl *a* molecules in the close vicinity of Cu-Pheo subunit in mixed aggregates. In these aggregates, the non-coherent hot migration of localized exciton within t_{HM}~10-20 ps over the distances up to R_{HM}~180 Å may even strengthen the quenching effect (see Figure 8B) compared to that found for porphyrin chemical dimers and triads/pentads where the energy transfer is not so fast and effective. It should be noted in this respect, that the theory (assuming that the Born-Oppenheimer approximation is valid for the aggregate) predicts that in the case of Chl a (or PChl a)-dioxane aggregates there is usually little overlap between the electronic wave functions of the neighboring molecules.[89] In means, that the exchange effects are not

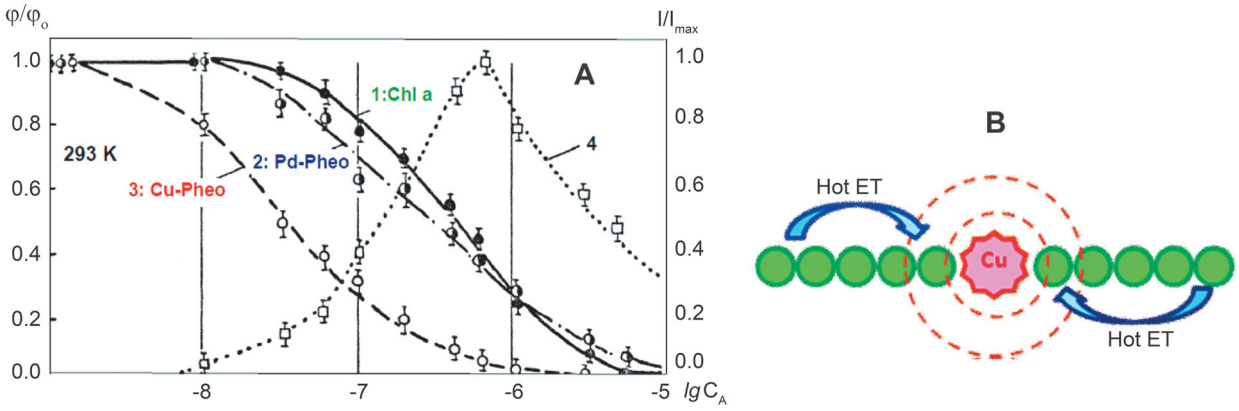

Figure 8. **A**: Dependence of the relative quantum efficiency (φ/φ_0) of fluorescence for protochlorophyll *a* aggregate (λ_{exc}=460 nm, λ_{det}=630 nm) upon mixed association with chlorophyll *a* (1), Pd-pheophytin *a* (2) and Cu-pheophytin *a* (3) being observed at the increase of the molar concentration of Chl *a*, Pd-Pheo and Cu-Pheo (C_A) to the initial solution of protochlorophyll (C_0=1×10^{-5} M). 4 – relative intensity (I/I_{max}) of chlorophyll *a* fluorescence (λ_{exc}=693 nm, λ_{det}=693 nm) in mixed aggregates with protochlorophyll *a*. **B**: Scheme of d-π exchange distant effects in mixed aggregates caused by Cu ion of Cu-pheophytin *a* and enhanced by "hot" energy transfer among aggregated host protochlorophyll *a* molecules.

excluded. Additionally, the semiempirical CI method treats (Chl *a*-dioxane)*n* aggregates and defines their spectroscopic properties according to the wave functions of the supermolecule.[89] These wave functions contain the effects from the linker molecules in the transitions involved and may, for instance, include also exchange d-π effects influence of the close (with interplane distance of about 7 Å) neighboring Pd-Pheo molecules. Our results suggest that the orbital overlap between the chromophores (Chl *a* or PChl *a,* and Cu-Pheo molecules, in the given case) may play an important role in determining spectral and the energy relaxation properties of these complexes.

Tuning Electronic States of CdSe/ZnS Quantum Dot by One Cu-Porphyrin Molecule

Recently, we have shown that "bottom-up" approach based on self-assembly principles defines a strategy of the formation of organic-inorganic nanoassemblies containing colloidal semiconductor CdSe or CdSe/ZnS quantum dots (QD) of various sizes and heterocyclic molecules (like *meso*-pyridyl substituted porphyrins in the given case).[29,90-99,123] Structures of QDs and porphyrin molecules as well as necessary details explaining the formation of nanoassemblies "QD-Porphyrin" are shown in Figure 9. The results described below concern to the analysis of the interaction between semiconductor CdSe/ZnS quantum dots and surface attached porphyrin molecules (free base and Cu-complex) in order to evaluate the influence of tetrapyrrolic macrocycle on pathways and mechanisms of exciton relaxation in "QD – Cu-porphyrin" nanoassemblies. More concretely, we will present our recent findings on "CdSe/ZnS QD – Cu-porphyrin" nanoassemblies showing that self-assembly of only one Cu-porphyrin molecule with one CdSe/ZnS quantum dot modifies not only the photoluminescence (PL) intensity of QD but creates new energetically clearly distinguishable electronic states opening additional effective relaxation pathways.

Comparative experiments on alone of TOPO-capped CdSe/ZnS QDs (d_{CdSe}=3.0 nm, two ZnS monolayers n_{ZnS}=2) and "QD-Porphyrin" nanoassemblies with participation of H_2P and/or CuP molecules have been performed in toluene at 293 K and in a methylcyclohexane/toluene (6:1) mixture in a temperature range from 77 K to 300 K. For single QDs measurements, the sample preparation was done by spin coating a ~$(1\div5)\cdot10^{-11}$ M solution of the QD onto a Si/SiO_2 (100 nm thick SiO_2) surface.[97,100,101]

We have quantitatively discriminated for the first time, that the major part of the observed PL strong quenching for CdSe/ZnS QD in "QD-Porphyrin" nanoassemblies can be understood in terms of the electron tunneling across the ZnS shell in the conditions of quantum confinement, and the minor part (10-15 %) of the QD PL quenching is caused by Foerster resonance energy transfer (FRET) QD→porphyrin.[90,91,93–97,123] Instead, the interaction of porphyrin molecules with QD leads to the inhomogeneous surface dynamics for

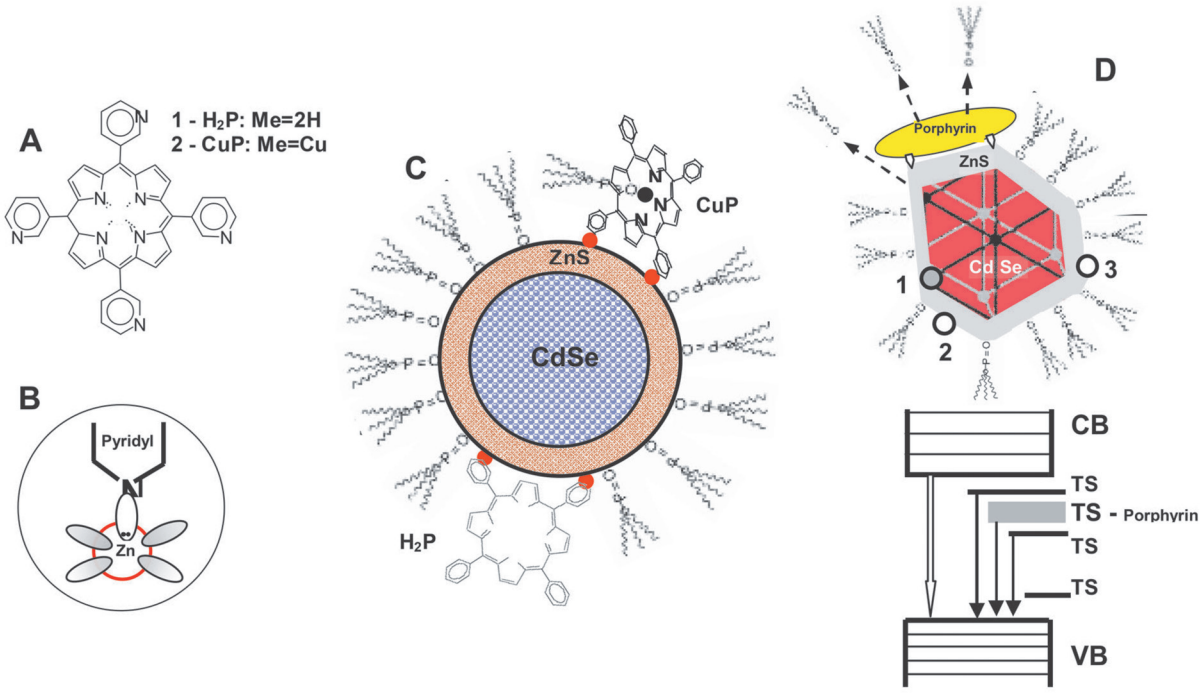

Figure 9. A: Chemical structures of 5,10,15,20-*meso*-*meta*-pyridyl porphyrins [free base H_2P (**1**) and CuP (**2**)]. **B**: Coordination scheme of porphyrins attachment to the ZnS shell via pyridyl N…Zn interaction. **C**: mutual arrangement of H_2P and CuP molecules with respect to the QD surface. Nitrogen lone pair orbitals (participating in Zn-N coordination) are indicated by a (red) dot. Capping ligands, trioctylphosphine oxide molecules (TOPO) are depicted also. Additional extra-ligation of TOPO molecule to the central Cu atom of CuP molecule is shown also (see explanation in the text). **D:** Schematic presentation of "QD-Porphyrin" nanoassembly as well as arbitrary excitonic and trap states (TS) and main relaxation pathways. An induced ligand (TOPO) detachment is shown by dashed arrows. 1 is a hole trap, 2 and 3 are electron traps. Partly adopted from refs. [99,123]

semiconductor QDs and the non-FRET quenching of QD PL in nanoassemblies might be related to few possible reasons: i) depletion of capping ligand TOPO molecules by the respective porphyrin molecules, ii) creation or redistribution of QD surface trap states, iii) low temperature reconstruction of capping ligand layer perturbed by attached porphyrin, etc. Correspondingly, using porphyrins (especially *meso*-pyridyl substituted H_2P and CuP) attaching with QD surface, one may tune the electronic states of CdSe/ZnS QD and control luminescent properties of nanoassemblies. Interestingly, for this tuning the PL properties of QDs, it does not need a full exchange of the ligand shell, but it works already upon attachment of very few dye molecules.[99] Below it will be comparatively shown it for "QD-CuP" and "QD-H_2P" nanoassemblies.

For a given TOPO-capped CdSe/ZnS QD (d_{CdSe}=2.6 nm, 2 monolayers ZnS) in toluene at 293 K, the results of QD PL quenching in nanoassemblies obtained with CuP molecules have been compared with those measured with H_2P, thus changing the spectral overlap integral values by 2 times ($J(\nu)=7.10\cdot10^{-14}$ $cm^6\cdot M^{-1}$ for CuP and $J(\nu)=3.65\cdot10^{-14}$ $cm^6\cdot M^{-1}$).[91,94] Nevertheless, Figure 10A shows that upon increasing the molar ratio x, QD PL quenching is nearly the same for CuP and H_2P, respectively. It means that the contribution of FRET (QD→porphyrin) to the total QD PL quenching in "QD-Porphyrin" nanoassemblies containing various porphyrin molecules is not the only and even not a major reason. In addition, in contrast to porphyrin heterodimers and multiporphyrin complexes (pentads, triads, *etc*.) containing Cu-porphyrin subunit (discussed above), any additional PL quenching caused by exchange d-π interactions is not observed in the case of QDs. It may be connected with a different nature of excitonic QD states which are not sensitive to unpaired d-electron of Cu ion in surface attached CuP molecules. Nevertheless, in low temperature experiments and upon QD PL decays analysis some specificity of the CuP influence on QD PL with respect to H_2P is found.

We have carried out the comparative temperature experiments for nanoassemblies based on TOPO capped CdSe/ZnS QD of one type with attached CuP and H_2P molecule at a relative molar ratio $x=[C_{Porphyrin}]/[C_{QD}]=1$ (Figure 10B). Temperature variation and related changes in emission intensities for pure QD (curve 1, Figure 10B) reveal sharp changes of TOPO ligand shell structure in a narrow temperature range ($T_{crit}\approx220$ K) for this surfactant (the so-called "phase transition").[96,99,123] It should be noted that T_{crit} is significantly higher than the temperature of the glass transition for the solvent mixture (T_{glass}=151.6 K). It is seen from Figure 10B also that at the same conditions, PL intensity for QD in "QD-CuP" and "QD-H_2P" nanoassemblies shows again a "kink" (curves 2 and 3), which, however, is now much more pronounced for CuP (curve 3) compared with both pure QD and QD-H_2P (curves 1 and 2). We conclude from temperature experiments, that the ligand phase transition perturbed by attached porphyrin molecule has impact on the QD core structure and exciton-phonon coupling. It is evident, that dye attachment enhances the PL decrease at the phase transition temperature, and the amplification is strongest for CuP molecules.

We like to address the question why are effects of nanoassembly formation more strongly pronounced at low temperatures for CuP as compared to H_2P though both porphyrins cause very similar PL quenching at room temperature. An intriguing explanation is outlined in Figure 9C and is probably connected with the following. It was found by picosecond transient absorption and nanosecond resonance Raman scattering that the triplet state of Cu-porphyrins is efficiently quenched by oxygen- or nitrogen-containing organic molecules.[53,124] Recently, based on X-ray diffraction crystallography data[125] it was shown that axial coordination of Cu(II)-porphyrin molecules (including also Cu-*tetra*-pyridyl-porphyrin[126]) ligation takes place via the formation of Cu···N or Cu···O bonds also in the ground state via five- or six-fold coordination depending on solvent and temperature. The ligation effects for Cu(II)-porphyrins should become stronger upon temperature lowering. TOPO molecules belong to the class of ligands which are able to form CuP-TOPO complexes. Following this conjecture, a CuP-TOPO complexation being five- or even six-coordinated at low temperatures may due to steric hindrance change the number of QD capping TOPO ligands considerably resulting in a displacement of the surrounding TOPO leading to a major distortion of the ligand shell close to the QD surface as is shown in Figure 9C.

Finally, consider the peculiarities of QD PL decay in "QD-CuP" (1:1) nanoassemblies. For these nanoassemblies, QD PL decays are multiexponential within the whole PL band both at room and low temperature, and measured mean decay times $\langle\tau\rangle$ slightly change upon variation of detection wavelengths. At 293 K, the mean decay shortening from $\langle\tau\rangle\approx14.5$ ns for pure QDs down to $\langle\tau\rangle\approx11.9$ ns for nanoassemblies is a direct evidence of OD PL quenching in nanocomposites due to both the electron tunneling and FRET. The temperature lowering down to 77 K leads to the strong shortening of mean $\langle\tau\rangle$ values down to ~8 ns.[99] At least 3 exponential functions (with decay times $\tau_1\leq1$ ns, $\tau_2\approx4-7$ ns and $\tau_3\approx10-18$ ns) are needed within our time resolution of 0.2 ns to approximate the PL decay for ensemble experiments (Figure 11A). Evaluation of single QD shows also a multi-exponential PL decay at each identified PL intensity (Figure 11B).[99] These results clearly show that low PL intensities correlate with short PL decay times, especially in the red part of the QD PL band.

The interpretation of QD PL decay results is also connected with TOPO capping layer phase transition perturbed by attached porphyrin molecules. The existence of additional PL quencher (attached CuP molecules) in this case may influence non-directly on the relative position of excitonic and trap states of QD itself upon temperature lowering as well as form the competitive non-radiative channels connected with CuP molecules. These findings prove that we are dealing, besides spectral broadening related to the size distribution of QDs, with an inhomogeneity of PL energies caused by the presence of various electronic states including trap states formed by CuP attachment (Figure 9D) which manifests itself in a large variation of PL decay times τ_i.

Concluding, the combination of ensemble and single QD experiments allows for a detailed complex analysis of the PL of QDs in CdSe/ZnS-Porphyrin nanoassemblies embedded in a glass matrix. In both cases, namely ensemble and time averaged single QD detection, electronic states of different nature with varying PL energies and decay

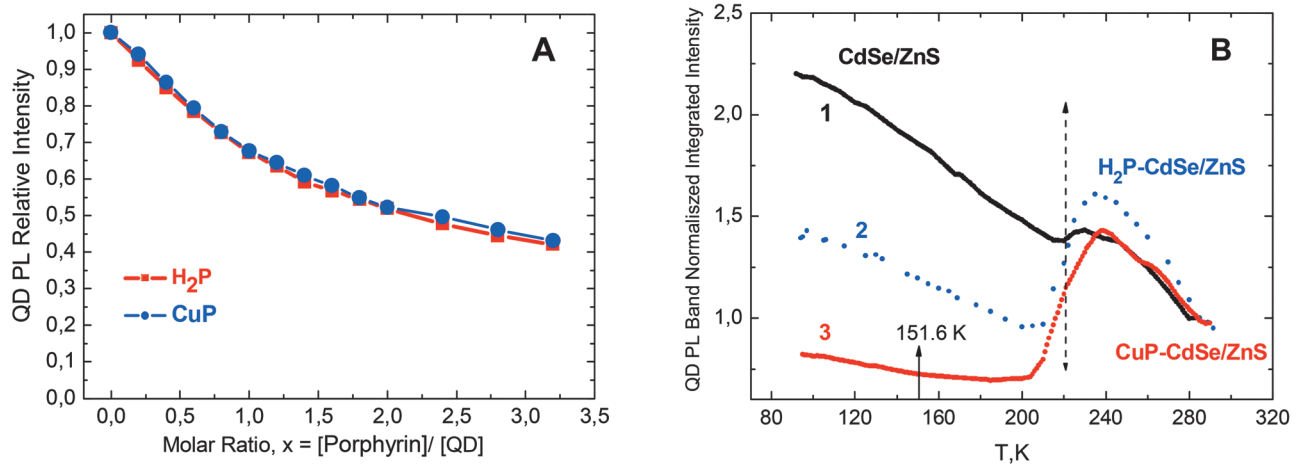

Figure 10. A: Photoluminescence quenching for TOPO-capped CdSe/ZnS QDs upon titration by H_2P and CuP molecules in toluene at 295 K) for various attached porphyrin molecules. d_{CdSe}=2.6 nm, 2 monolayers ZnS, λ_{exc}=440 nm, λ_{reg}=554 nm. **B**: Temperature dependence of normalized QD PL intensity ratio, for TOPO-capped CdSe/ZnS (1) as well as for QDs in H_2P-CdSe/ZnS (2) and CuP-CdSe/ZnS (3) nanoassemblies at molar ratio x=1 in a methylcyclohexane-toluene (6:1) mixture for λ_{exc}=450 nm. Temperature T_{crit}≈220 K (phase transition assigned to the capping TOPO layer) are indicated by dashed arrow. The temperature of the glass transition for the methylcyclohexane/toluene (6:1) mixture at 151.6 K is shown by an arrow (full line). Partly adopted from refs.[94,99,123]

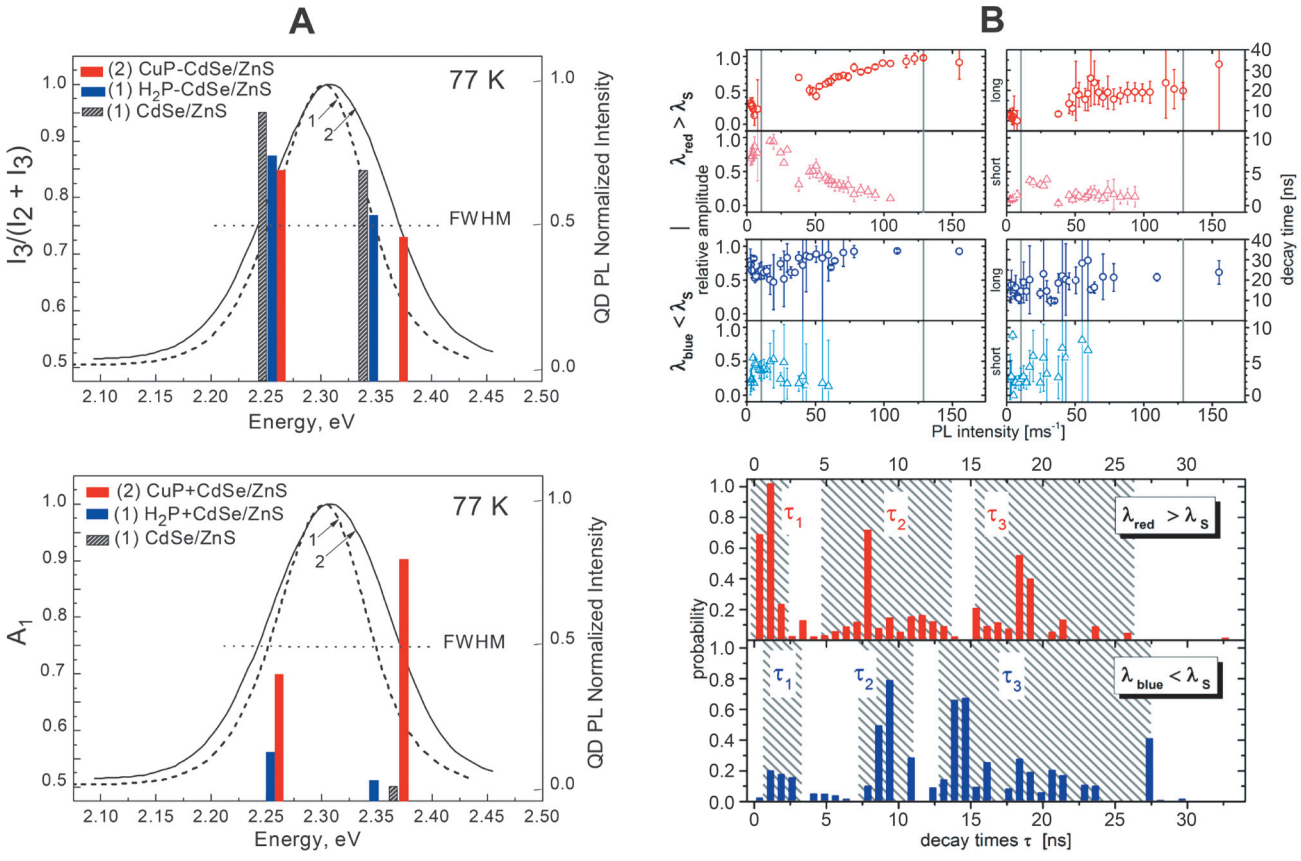

Figure 11. QD photoluminescence analysis for ensemble experiments (**A**) single quantum dots (**B**) based on experimental results presented in [99]. **A**: Relative PL intensities $I_3/(I_2+I_3)$ (top) and normalized amplitudes A_1 (bottom) for solutions of pure CdSe/ZnS QDs and QDs in "QD-CuP" or "QD-H_2P" nanoassemblies at 77 K. Normalized QD PL bands are shown as broken lines for pure CdSe/ZnS (1) or QDs in H_2P-CdSe/ZnS (1) and as full lines for CuP-CdSe/ZnS (2) nanoassemblies at 77 K. FWHM is the full width of half-maximum of the corresponding bands. **B**: Variations of PL decay times (two-exponential fits) during a blinking time trace for single CdSe/ZnS QDs on a quartz substrate at room temperature upon detection in the red and blue range of the PL band, respectively. Data are presented for amplitudes and lifetimes detected for the PL of one single QD in 2 different spectral detection channels (top) and for 20 single QDs depending on the spectral detection channel (bottom). "Grouping" of decay times into 3 typical time regimes τ_i is indicated by shaded areas.

dynamic are subsequently explored on slow time scales typical for blinking phenomena which are buried but nevertheless present in ensemble experiments. These results evidently show that already one attached CuP porphyrin molecule causes not only QD PL quenching but also changes the energy landscape of the QD PL noticeably, and temperature controls the energetic ordering of QD surface states.

Conclusions

It is clear that for any given multicomponent nanostructure the main problem is the understanding presumably of how the multiple components by various nature and composition may interact and function as a whole in order to predict its possible applications. Here, we discussed some relatively rare relaxation processes in multicomponent nanostructures including Cu containing tetrapyrrolic macrocycles which make these nanoassemblies more special. This discussion is based on steady-state, picosecond time-resolved measurements and single objects detection, including temperature range 77 – 293 K in some cases. The important question under discussion was: what happens with excited states of nanoassembly subunits of various nature and morphology being coupled with adjacent Cu-porphyrins. Correspondingly, the subject of a discussion were: porphyrin chemical dimers with various spacers, self-organized multiporphyrin complexes (pentads and larger complexes with well-defined geometry), polymeric ordered aggregates of photosynthetic pigments (chlorophyll and protochlorophyll) and nanoassemblies based on semiconductor CdSe/ZnS quantum dots and tetra-*meso*-pyridyl substituted porphyrins (free base and Cu-complex).

It has been evaluated that the electronic excitation energy relaxation in Cu-porphyrin containing hybrid chemical dimers with various spacers may be connected with few reasons (depending on the dimer structure, nature of spacer and energetic properties of interacting counterparts): i) the increase of the non-radiative deactivation of excited states for the dimer half not containing central Cu ion (due to exchange d-π effects); ii) ET process from thermally equilibrated "trip-doublet" ($^2T_1$) and "trip-quartet" ($^4T_1$) states of Cu-porphyrin half to the locally excited T_1 state of porphyrin free base half; iii) the formation of short-lived radical ion pair formed by the photoinduced electron transfer from the excited singlet precursor; iv) exchange resonance T-T energy transfer in dimers of both Cu-porphyrins.

Using low-temperature experiments we found that long-distant exchange d-π effects manifest themselves also in more complex multiporphyrin self-assembled arrays such as pentads (based on two chemical dimers $(ZnOEP)_2Ph$ coordinatively coupled by Cu-tetra-*meta*-pyridyl porphyrin) and larger complexes (composed of chemical trimer $(ZnOEP)_3Ph_2$, porphyrin free base and Cu-complex) with well-defined geometry. In these complexes, fluorescence of all components is quenched in the presence of Cu-containing

We have shown that a strong quenching of protochlorophyll fluorescence being observed in mixed ordered aggregates with Cu-pheophytin (at even small molar ratios PChl:Cu-Pheo=1000 – 100) is definitely connected with exchange d-π effects influence on the neighboring PChl *a* molecules in the close vicinity of Cu-Pheo subunit in mixed aggregates. In these aggregates, the non-coherent hot migration of localized exciton within t_{HM}~10 – 20 ps over the distances up to R_{HM}~180 Å may even strengthen the quenching effect compared to that found for porphyrin chemical dimers and triads/pentads where the energy transfer is not so fast and effective.

Finally, in contrast to porphyrin heterodimers and multiporphyrin complexes (pentads, triads, aggregates, *etc*.) containing Cu-porphyrin subunit, any additional PL quenching caused by exchange d-π interactions is not observed in the case of "QD-CuP" nanoassemblies. Instead, using the combination of ensemble and single QD experiments together with low-temperature experiments and PL decay analysis for "QD-CuP" nanoassemblies, it was experimentally proven for the first time that already one attached Cu-porphyrin molecule on QD surface causes not only QD PL quenching but also changes the energetic ordering of electronic surface states of the QD significantly. Especially below the "phase transition" of TOPO ligands, PL energies depend critically on the surface-attached Cu-porphyrin. On the basis of a combination of ensemble and single molecule spectroscopy of nanoassemblies, we have shown that single functionalized molecules (Cu-porphyrin in our case) can be considered as extremely sensitive probes for studying the complex interface physics and exciton relaxation processes in QDs.

Considering the vast amount of current nanotechnological applications in diverse areas such as bioimaging, nanophotonics or solar energy conversion, and the need for reliable methods for the proper characterization of nanostructures of various composition and morphology, we believe that the submitted manuscript will be of interest for a wide number of readers of MHC.

Acknowledgements. I like to thank Dr. A. Shulga (B.I. Stepanov Institute of Physics, National Academy of Sciences, Minsk, Belarus) for synthesis and identification of all compounds being studied. Data related to spectral-kinetic characterization of porphyrins and their chemical dimers have been obtained by Drs. V. Knyukshto and A. Stupak (Institute of Physics, Minsk). I also thank Dr. Habil. E. Sagun for fruitful discussion. Especial thanks to Prof. C. von Borczyskowski (TU Chemnitz, Germany) for fruitful long-standing collaboration upon studying various types of organic and organic-inorganic nanoassemblies. This work was funded by the Volkswagen Foundation (VW Grant I/79435 within the Priority Program "Physics, Chemistry and Biology with Single Molecules"), Project DFG Priority Unit FOR 877, Sachsischen Forschengruppe «From Local Constraints to Macroscopic Transport», the Belorussian State Programs for Scientific Research "Convergence 3.2.08 – Photophysics of Bioconjugates, Semiconductor and Metallic Nanostructures and Supramolecular Complexes and Their Biomedical Applications" and "Convergence–2020 3.03 – Nanoassemblies "semiconductor quantum dots-porphyrin nanotubes and their interaction with plasmonic structures: self-assembly principles, morphology, relaxation processes and possible applications".

References

1. Lehn J.-M. *Angew. Chem., Int. Ed. Engl.* **1990**, 29, 1304–1319.
2. Whitesides G.M., Grzybowski B. *Science* **2002**, *295*, 2418–2421.
3. *Handbook of Molecular Self-Assembly: Principles, Fabrication and Devices* (Peinemann K.-V., Barboiu M., Eds.) Pan Stanford Publishing Co. Singapore: Pte. Ltd., **2012**.
4. Tietz C., Jelezko F., Gerken U., Schuler S., Schubert A., Rogl H., Wrachtrup J. *Biophys. J*. **2001**, *81*, 556–562.
5. Cogdell R.J., Gall A., Koehler J. *Quarterly Reviews of Biophysics* **2006**, *39,* 227–324.
6. Gall A., Sogalia E., Gulbinas V., Ilioaia O., Robert B., Valkunas L. *Biochim. Biophys. Acta* **2010**, *1797*, 1465-1469.
7. Valkunas L., Trinkunas G., Chmeliov J., Ruban A.V. *Phys. Chem. Chem. Phys.* **2009**, *11*, 7576–7584.
8. Freiberg A., Trinkunas G. In: *Unraveling the Hidden Nature of Antenna Excitations* (Laisk A., Nedbal L., Govindjee, Eds.) Amsterdam: Springer Science+Media B.V., **2009**, p. 55–82.
9. Unterkofler S., Pflock T., Southall J., Cogdell R.J., Koehler J. *ChemPhysChem* **2011**, *12*, 711–716.
10. *Handbook of Porphyrin Science: With Application to Chemistry, Physics, Materials Science, Engineering, Biology and Medicine* (Kadish K.M., Smith K.M., Guilard R., Eds.) Singapore: World Scientific Publishing Co. Pte. Ltd, **2012**, Vol. 22.
11. Lee J.-E., Yang, J., Gunderson V.L., Wasielewski M.R., Kim D. *J. Phys. Chem. Lett.* **2010**, *1*, 284–289.
12. Chen M., Scheer H. *J. Porphyrins Phthalocyanines* **2013**, *17*, 1–15.
13. *Multiporphyrin Arrays: Fundamentals and Applications* (Kim D., Ed.) Singapore: Pan Stanford Publishing Pte. Ltd., **2012**, 612 p.
14. Cao G., Wang Y. *Nanostructures and Nanomaterials: Synthesis, Properties and Applications*. New York: World Scientific Series in Nanoscience and Nanotechnology, **2011**, 2nd Edition, Vol. *2*, 596 p.
15. Bottari, G., Suanzes, J.A., Trukhina, O., Torres T. *J. Phys. Chem. Lett.* **2011**, *2*, 905–913.
16. Colvin M.T., Ricks A.B., Scott A.M., Smeigh A.L. Carmieli R., Miura T., Wasielewski M.R. *J. Am. Chem. Soc*. **2011**, *133*, 1240–1243.
17. Zenkevich E.I. *Macroheterocycles* **2014**, 7, 103–121.
18. Zenkevich E.I., von Borczyskowski C. *J. Porphyrins Phthalocyanines* **2014**, *18*, 1–19.
19. Langlois A., Xu H.-J., Karsenti P.-L., Gros C.P., Harvey P. *J. Porphyrins Phthalocyanines* **2015**, *19*, 427–441.
20. Wiwatowski K., Dużyńska A., Świniarski M., Szalkowski M., Zdrojek M., Judek J., Mackowski S., Kaminska I. *J. Luminescence* **2016**, *170*, 855–859.
21. Kilin D., Zenkevich E., von Borczyskowski C. In: *Proc. Int. Conf. "Nanomeeting-2015". Physics, Chemistry and Applications of Nanostructures. Reviews and Short Notes* (Borisenko V.E., Gaponenko S.V., Gurin V.S., Kam C.H., Eds.) London: World Scientific Publishing Co., **2015**, 14–17.
22. Sheinin V.B., Shabunin S.A., Bobritskaya E.V., Koifman O.I., Zenkevich E.I., Strekal N.D., Gogoleva S.D. Formation Principles, Optical Properties and Surface Enhanced Raman Scattering for Porphyrin Nanotubes Fixed on Plasmonic Resonance Particles. In: *Proc. Int. Conf. "Nanomeeting-2015". Physics, Chemistry and Applications of Nanostructures. Reviews and Short Notes* (Borisenko V.E., Gaponenko S.V., Gurin V.S., Kam C.H., Eds.) London: World Scientific Publishing Co., **2015**, 338–341.
23. Nicolini C. *Nanotechnology and Nanobiosciences*, *Ch. 1, Nanoscale Materials*. Pan Stanford Series on Nanobiotechnology, **2010**, Vol. 1.
24. *Encyclopedia of Nanotechnology* (Bhushan B., Ed.). Heidelberg: Springer Science. Business Media B.V, **2012**.
25. Bawa R., Audette G.F., Rubinstein I. *Handbook of Clinical Nanomedicine: Nanoparticles, Imaging, Therapy, and Clinical Applications Series: Pan Stanford Series on Nanomedicine.* Singapore: Pan Stanford CRS, **2016**.
26. *Handbook of Porphyrin Science: With Applications to Chemistry, Physics, Material Science, Engineering, Biology and Medicine* (Kadish K., Smith K.M., Guilard R., Eds.) Abingdon, UK: World Scientific Publishing Ltd., **2010**, Vols. 1, 4, 10.
27. Zenkevich E.I., von Borczyskowski C. Multiporphyrin Self-Assembled Arrays in Solutions and Films: Thermodynamics, Spectroscopy and Photochemistry. In: *Handbook of Polyelectrolytes and Their Applications* (Tripathy S.K., Kumar J., Nalwa H.S., Eds.) USA: American Scientific Publishers. **2002**, Vol. 2, Ch. 11, 301–348.
28. Chambrier I., Banerjee C., Remiro-Buenamañana S., Chao Y., Cammidge A.N., Bochmann M. *Inorg. Chem*. **2015**, *54*, 7368−7380.
29. Zenkevich E., von Borczyskowski C. Surface Photochemistry of Quantum Dot-Porphyrin Nanoassem-blies for Singlet Oxygen Generation. In: *Photoinduced Processes at Surfaces and in Nanomaterials* (Kilin D., Ed.). ACS Symposium Series, **2015**, Vol. 1196, Ch. 12, 235–272.
30. Hadar I., Halivni S., Even-Dar N., Faust A., Banin U. *J. Phys. Chem. C.* **2015**, *119*, 3849−3856.
31. Haghi A.K., Thomas S., Pourhashemi A., Hamrang A., Klodzinska E. *Nanomaterials and Nanotechnology for Composites: Design, Simulation and Applications.* Apple Academic Press, **2015**.
32. Osifeko O., Nyokong T. *Dyes Pigm.* **2016**, *131*,186–200.
33. Zenkevich E.I., Shulga A.M., Chernook A.V., Gurinovich G.P., Sagun E.I. Covalently Linked Porphyrin Dimers as Model Systems of the Photosynthetic Special Pair: Spectroscopy, Energetics and Photochemistry. In: *Light in Biology and Medicine* (Douglas R.H., Moan J., Ronto G., Eds.). New York and London: Plenum Press, **1991**, Vol. 2, 337–344.
34. Zenkevich E.I., Shulga A.M., Chernook A.V., Sagun E.I., Gurinovich G.P. *Proc. Indian Acad. Sci., Chem. Sciences* **1995**, *107*, 795–802.
35. Burrell A.K.,Wasielewski M.R. *J. Porphyrins Phthalocyanines* **2000**, *4*, 401–411.
36. Beyler M., Flamigni L., Heitz V., Sauvage J.-P., Ventura B. *Photochem. Photobiol.* **2014**, *90*, 275–286.
37. Oksanen J.A.I., Zenkevich E.I., Knyukshto V.N., Pakalnis S., Hynninen P.H., Korrpi-Tommola J.E.I. *Biochim. Biophys. Acta, Bioenergetics* **1997**, *1321*, 165–178.
38. Zenkevich E.I., von Borczyskowski C.W. Formation Principles and Excited States Relaxation in Self-Assembled Complexes: Multiporphyrin Arrays and "Semiconductor CdSe/ZnS Quantum Dot-Porphyrin" Nanocomposites. In: *Handbook of Porphyrin Science with Application to Chemistry, Physics, Materials Science, Engineering, Biology and Medicine*. (Kadish K., Smith K.M., Guilard R., Eds.) Singapore: Scientific Publishing Co. Pte. Ltd., **2012**, Vol. *22*, Ch. 104, 68–159.
39. Camus J.-M., Langlois A., Aly S., Guilard R., Harvey P.D. *J. Porphyrins Phthalocyanines* **2013**, *17*, 722–732.
40. Subbaiyan N.K., D'Souza F. *J. Porphyrins Phthalocyanines* **2013**, *17*, 733–749.
41. Terazono Y., Kodis G., Chachisvilis M., Cherry B.R., Fournier M., Moore A., Moore T.A., Gust D. *J. Am. Chem. Soc.* **2015**, *137*, 245-258.
42. Forster Th. In: *Modern Quantum Chemistry*. New York-London: Acad. Press, **1965**, Vol. *3*, 93-127.
43. Agranovich V.M., Galanin M.D. *Electronic Excitation Energy Transfer in Condensed Media.* Moscow: Nauka, **1977**.

44. Dexter D.L. *J. Chem. Phys.* **1953**, *21*, 836–850.
45. Ermolaev V.L., Bodunov E.N., Sveshnikova E.B., Shakhverdov T.A. *Non-Radiative Electronic Excitation Energy Transfer*. Leningrad: Nauka, **1977**. 311 p. (in Russ) [Ермолаев В.Л. *Безызлучательный перенос энергии электронного возбуждения*. М.: Наука, **1977**. 311 с.].
46. Marcus R.A. *Rev. Modern Phys*. **1993**, 65, 599–610.
47. Sutin N. In: *Electron Transfer in Inorganic, Organic, and Biological Systems (*Bolton J.M., Mataga N., McLendon J., Eds.). Washington: Am. Chem. Soc., CSC Symposium Series, **1991**, Vol. 2, p. 25–47.
48. Jortner J., Bixon M., Heitele H., Michel-Beyerle M.E. *Chem. Phys. Lett*. **1992**, *1997*, 131-146.
49. Clayton A.H.A., Scholes G.D., Ghiggino K.P., Paddon-Row M.N. *J. Phys. Chem.* **1996**, *100*, 10912–10918.
50. Bixon M., Jortner J., Michel-Beyerle M.E. *Chem. Phys*. **1995**, *197*, 389-404 and references therein.
51. Davis W.B., Wasielewski M.R., Ratner M.A., Mujica V., Nitzan A. *J. Phys. Chem*. **1997**, *101*, 6158–6164.
52. Ake R.L., Gouterman M. *Theoret. Chim. Acta*. **1969**, *15*, 20–29.
53. Kim D., Holten D., Gouterman M. *J. Am. Chem. Soc*. **1984**, *106*, 2793–2798.
54. Kobayashi T., Huppert D., Straub K.D., Rentzepis P.N. *Photochem. Photobiol.* **1979**, *70*, 1720–1726.
55. Cunningham K.L., McNett K.M., Pierce R.A., Davis K.A., Harris H.H., Falck D.M., McMillin D.R. *Inorg. Chem.* **1997**, *36*, 608.
56. McMillin D.R., McNett K.M. *Chem. Rev.* **1998**, *98*, 1201.
57. Dzhagarov B.M., Chirvony V.S., Gurinovich G.P. In: *Laser Picosecond Spectroscopy and Photochemistry of Biomolecules* (Letokhov V.S., Ed.) Moscow: Nauka, **1987**. p. 181–212 (in Russ.) [Джагаров Б.М., Чирвоный В.С., Гуринович Г.П. *Пикосекундная спектроскопия и фотохимия биомолекул* (Летохов В.С., ред.). М.: Наука, **1987**. с.180-212].
58. Jeung S.C., Kim D., Cho D.W., Yoon M. *J. Phys*. *Chem.* **1995**, *99*, 5826–5833.
59. McGlynn S.P., Azumi T., Kinoshita M. *Molecular Spectroscopy of the Triplet State.* New Jersey: Prentice-Hall Inc. Englewood Cliffs, **1969**, Ch. 8. p. 305–348.
60. Sagun E.I., Zenkevich E.I., Knyukshto V.N., Shulga A.M. *Opt. Specktrosk.* **2005**, *99*, 575–588 (in Russ.).
61. Ponomarev G.V., Shul'ga A.M. *Dokl. Akad. Nauk SSSR* **1983**, *271*, 365–367 (in Russ.).
62. Gurinovich G.P., Zenkevich E.I., Sagun E.I., Shulga A.M. *Opt. Specktrosk.* **1984**, *56*, 1037–1043 (in Russ.).
63. Gurinovich G.P., Zenkevich E.I., Shulga A.M., Sagun E.I., Mauring K., Suisalu A. *Zh. Prikl. Spektrosk.* **1984**, *41*, 446–450 (in Russ.).
64. Zenkevich E.I., Shulga A.M., Gurinovich G.P., Sagun E.I. *Zh. Prikl. Spektrosk.* **1985**, *42*, 207–213 (in Russ.).
65. Zenkevich E.I., Shulga A.M., Chernook A.V., Sagun E.I., Gurinovich G.P. *Khim. Fizika* **1989**, *8*, 842–853 (in Russ.).
66. Mauring K., Suisalu A., Kikas J., Zenkevich E.I., Chernook A.V., Shulga A.M., Gurinovich G.P. *J. Lumin.* **1995**, *64*, 141–148.
67. Zenkevich E.I., Shulga A.M., Chernook A.V., Gurinovich G.P *Zh. Prikl. Spektrosk.* **1986**, *45*, 790–796 (in Russ.).
68. Zenkevich E.I., Shulga A.M., Chernook A.V., Gurinovich G.P. *Chem. Phys. Lett*. **1984**, *109*, 306–311.
69. Zenkevich E.I., Chernook A.V., Shulga A.M., Sagun E.I., Gurinovich G.P. *Khim. Fizika* **1989**, *8*, 891–901 (in Russ.).
70. Chernook A.V., Zenkevich E.I., Shulga A.M. *Zh. Prikl. Spektrosk.* **1991**, *55*, 445–451 (in Russ.).
71. Chernook A.V. *Photonics of Bichromophores on the Basis of Pigments and Dyes*. PhD Thesis. Minsk: Institute of Molecular and Atomic Physics, **1990**. 110 p.
72. Zenkevich E.I., Chernook A.V., Shulga A.M., Pershukevich P.P., Gurinovich G.P., Sagun E.I. *Khim. Fizika* **1991**, *10*, 1183–1191 (in Russ.).
73. Starukhin A., Zenkevich E., Shulga A., Chernook A. *J. Lumin*. **1996**, *68*, 313–323.
74. Chernook A.V., Shulga A.M., Zenkevich E.I., Rempel U., von Borczyskowski C. *J. Phys. Chem*. **1996**, *100*, 1918–1926.
75. Knyukshto V., Zenkevich E., Sagun E., Shulga A., Bachilo S. *Chem. Phys. Lett*. **1998**, *297*, 97–108.
76. Knyukshto V., Zenkevich E., Sagun E., Shulga A., Bachilo S. *J. Fluoresc.* **2000**, *10*, 55–68.
77. Chernook A.V., Rempel U., von Borczyskowski C., Zenkevich E.I., Shulga A. *Chem. Phys. Lett*. **1996**, *254*, 229–241.
78. Bachilo S., Willert A., Rempel U., Shulga A.M., Zenkevich E.I., von Borczyskowski C. *J. Photochem. Photobiol. A, Chemistry* **1999**, *126*, 99–112.
79. Sagun E.I., Zenkevich E.I., Knyukshto V.N., Shulga A.M., Starukhin D.A., von Borczyskowski C. *Chem. Phys.* **2002**, *275*, 211–237.
80. Zenkevich E.I., von Borczyskowski C., Shulga A.M. *J. Porphyrins Phthalocyanines* **2003**, *7*, 731–754.
81. Rempel U., von Maltzan B., von Borczyskowski C. *Pure Appl. Chem*. **1993**, *65*,1681–1685.
82. Rempel U., Meyer S., von Maltzan B., von Borczyskowski C. *J. Lumin*. **1998**, *78*, 97–110.
83. Zenkevich E.I., Willert A., Bachilo S.M., Rempel U., Kilin D.S., Shulga A.M., von Borczyskowski Ch. *Mater. Sci. Eng., C* **2001**, *18*, 99–111.
84. Zenkevich E.I., von Borczyskowski C., Shulga A.M., Bachilo S.M., Rempel U., Willert A. *Chem. Phys.* **2002**, *275*, 185–209.
85. Zenkevich E.I., Losev A.P., Kochubeev G.A., Gurinovich G.P. *J. Mol. Struct*. **1978**, *45*, 423–436.
86. Chirvonyi V.S., Zenkevich E.I., Gadonas R., Krasauskas V., Pelakauskas A. *J. Lumin.* **1990**, *45*, 392–396
87. Zenkevich E. *Photophysics of Concentrated Solutions of Pigments and Structurally-Organized Molecular Systems with Their Participation*. Doct. Habil. Thesis. Minsk: Institute of Physics, **1990**. 333 p.
88. Oksanen J.A.I., Zenkevich E.I., Knyukshto V.N., Pakalnis S., Hynninen P.H., Korrpi-Tommola J.E.I. *Biochim. Biophys. Acta, Bioenergetics* **1997**, *1321*, 165–178.
89. Linnanto J., Helenius V.M., Oksanen J.A.I., Peltola T., Garaud J.-L., Korppi-Tommola J.E.I. *J. Phys. Chem. A* **1998**, *102,* 4337–4349.
90. Zenkevich E., Cichos F., Shulga A., Petrov E., Blaudeck T., von Borczyskowski C. *J. Phys. Chem. B* **2005**, *109*, 8679–8692.
91. Zenkevich E.I., Blaudeck T., Shulga A.M., Cichos F., von Borczyskowski C. *J. Lumin*. **2007**, *122-123*, 784–788.
92. Kilin D.S., Tsemekhman K., Prezhdo O.V., Zenkevich E.I., von Borczyskowski C. *J. Photochem. Photobiol., A* **2007**, *190*, 342–354.
93. Blaudeck T., Zenkevich E., Cichos F., von Borczyskowski C. *J. Phys. Chem. C* **2008**, *112*, 20251–20257.
94. Zenkevich E.I., von Borczyskowski C. *Macroheterocycles* **2009**, *2*, 206–220.
95. Blaudeck T., Zenkevich E., Abdel-Mottaleb M., Szwaykowska K., Kowerko D., Cichos F., von Borczyskowski C. *ChemPhysChem* **2012**, *13*, 959–972.
96. Zenkevich E.I., Stupak A.P., Kowerko D., von Borczyskowski C. *Chem. Phys*. **2012**, *406*, 21–29.
97. Zenkevich E.I., Blaudeck T., Kowerko D., Stupak A.P., Cichos F., von Borczyskowski C. *Macroheterocycles* **2012**, *5*, 98–114.
98. Zenkevich E.I., Gaponenko S.V., Sagun E.I., von Borczyskowski C. *Rev. Nanosci. Nanotech.* **2013**, *2*, 184-207.
99. Zenkevich E., Stupak A., Göhler C., Krasselt C., von Borczyskowski C. *ACS Nano* **2015**, *9*, 2886-2903.

100. Kowerko D., Schuster J., Amecke N., Abdel-Mottaleb M., Dobrawa R., Würthner F., von Borczyskowski C. *Phys. Chem. Chem. Phys.* **2010**, *12*, 4112–4123.
101. Schmidt R., Krasselt C., Göhler C., von Borczyskowski C. *ACS Nano.* **2014**, *8*, 3506–3521.
102. Schwarz F.P., Gouterman M., Muljiami Z., Dolphin D. Bioinorg. Chem. **1972**, *2*, 1–32.
103. Anton J.A., Loach P.A., Govindjee *Photochem. Photobiol.* **1978**, *28*, 235–242.
104. Zenkevich E.I., Shulga A.M., Sagun E.I., Gurinovich G.P. In: *Proc. of XIX Union Meeting on Spectroscopy. Part III: Spectroscopy of Complex Molecules,* Tomsk, USSR, **1983**, 102–104.
105. Zenkevich E.I., Shulga A.M., Sagun E.I., Gurinovich G.P., Chernook A.V. *Teubner-Texte zur Physik*, Leipzig: BSB B.G.Teubner Verlagsgesselschaft, **1985**, *4,* 297–300.
106. Brookfield R.L., Ellul H., Harriman A. *J. Chem. Soc., Farad. Trans. II* **1985**, *81*, 1837–1848.
107. Ohno A., Ogasawara Y., Asano M., Kajii Y., Kaizu Y., Obi K., Kobayashi H. *J. Phys. Chem.* **1987**, *91*, 4269–4273.
108. Mialocq J.C., Gianotti C., Maillard P., Momenteau M. *Chem. Phys. Lett.* **1984**, *112*, 87–93.
109. Asano-Someda M., Kaizu Y. *Inorg. Chem.* **1999**, *38*, 2303–2311.
110. Hugerat M., Levanon H., Ojadi E., Biczok L., Linschitz H. *Chem. Phys. Lett.* **1991**, *181*, 400–406.
111. Hugerat M., Van der Est A., Ojadi E., Biczok L., Linschitz H., Levanon H., Stehlik D. *J. Phys. Chem.* **1996**, *100*, 495–500.
112. Asano-Someda M., Ichino T., Kaizu Y. *J. Phys. Chem. A* **1997**, *101*, 4484–4490.
113. Asano-Someda M., Van der Est A., Kruger U., Stehlik D., Kaizu Y., Levanon H. *J. Phys. Chem. A* **1999**, *103*, 6704–6714.
114. Toyama N., Asano-Someda M., Ichino T., Kaizu Y. *J. Phys. Chem. A* **2000**, *104*, 4857–4865.
115. Sagun E.I., Ganzha V.A., Dzhagarov B.M., Shulga A.M. *Khim. Fizika* **1991**, *10*, 477–484 (in Russ.).
116. Andreasson J., Kajanus J., Martinsson J., Albinsson B. *J. Am. Chem. Soc.* **2000**, *122*, 9844–9845.
117. Rempel U., Brunn R., von Borczyskowski C., Hugerat M. *SPIE Vol. 1921 Laser Spectroscopy of Biomolecules* **1992**, 122–130.
118. Zenkevich E.I., von Borczyskowski C. Photoinduced Relaxation Processes in Self-Assembled Nanostructures: Multiporphyrin Complexes and Composites "CdSe/ZnS Quantum Dot-Porphyrin". In: *Multiporphyrin Arrays: Fundamentals and Applications* (Kim D., Ed.). Singapore: Pan Stanford Publishing Pte. Ltd., **2012**, Ch. 5, 217–288.
119. Sagun E.I., Zenkevich E.I., Knyukshto V.N., Shulga A.M., Ivashin, N.V. *Opt. Specktrosk.* **2010**, *108*, 590–607 (in Russ.).
120. Kuciauskas D., Liddell P.A., Hung S.-C., Lin S., Stone S., Seely G.R., Moore A.L., Moore T.A., Gust D. *J. Phys. Chem. B*. **1997**, *101*, 429–440.
121. Wasielewski M.R. *Chem. Rev*. **1992**, 92, 435–461.
122. Khizhnyakov V.V., Tekhver Yu.I. *Izv. Akad. Nauk SSSR, Ser. Fiz.* **1975**, *39*, 1895–1899 (in Russ.).
123. Borczyskowski C., Zenkevich E. Formation Principles and Exciton Relaxation in Semiconductor Quantum Dot – Dye Nanoassemblies. In: *Quantum Dot Molecules. Lecture Notes in Nanoscale Science and Technology. Springer Series in Materials Science* (Wu J., Wang Z.M., Eds.). New York: Springer Science+Business Media, **2014**, Vol. 14, p. 77–148.
124. Apanasevich P.A., Gadonas R., Kvach V.V., Krasauskas V., Orlovich V.A., Chirvony V.S. *Khim. Fizika* **1988**, *7*, 21–32 (in Russ.).
125. Sinelshchikova A.A., Nefedov SE., Enakieva Yu.Yu., Gorbunova Yu.G., Tsivadze A.Yu., Kadish K.M., Chen P., Bessmertnykh-Lemeune A., Stern C., Guilard R. *Inorg. Chem*. **2013**, *52*, 999−1008.
126. Wang J.-Q., Ren C.-X., Weng L.-H., Jin, G.-X. *Chem. Commun*. **2006**, 162–164.

Received 12.05.2016
Accepted 17.05.2016